

UNCLASSIFIED

AD 411581

DEFENSE DOCUMENTATION CENTER

FOR

SCIENTIFIC AND TECHNICAL INFORMATION

CAMERON STATION, ALEXANDRIA, VIRGINIA



UNCLASSIFIED

NOTICE: When government or other drawings, specifications or other data are used for any purpose other than in connection with a definitely related government procurement operation, the U. S. Government thereby incurs no responsibility, nor any obligation whatsoever; and the fact that the Government may have formulated, furnished, or in any way supplied the said drawings, specifications, or other data is not to be regarded by implication or otherwise as in any manner licensing the holder or any other person or corporation, or conveying any rights or permission to manufacture, use or sell any patented invention that may in any way be related thereto.

CATALOGED BY DDC

AS AD No. ~~411581~~ 411581

411581

FINAL TECHNICAL SUMMARY REPORT

Report Date: June 14, 1963

May 1, 1962 to April 30, 1963

ORIGINAL CONTAINS COLOR PLATES: ALL DDC
REPRODUCTIONS WILL BE IN BLACK AND WHITE
ORIGINAL MAY BE SEEN IN DDC HEADQUARTERS

"VARIABLE ENERGY GAP DEVICE"

CONTRACT NR. DA-36-039-SC-89106

Placed By:

*U. S. Army Signal Research & Development
Laboratories, Fort Monmouth, New Jersey*

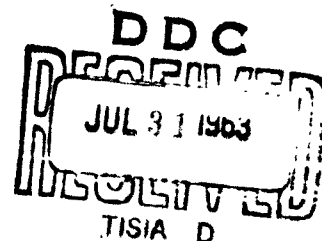


THE EAGLE-PICHER COMPANY

Chemicals & Metals Division,

Research Laboratories,

Miami, Oklahoma



NO. 075

ORIGINAL CONTAINED IN: ALL DDO
FOR: WHITE.
ORIGINAL DATE: 1963.

FINAL TECHNICAL SUMMARY REPORT

Covering the Period

May 1, 1962 to April 30, 1963.

"VARIABLE ENERGY GAP DEVICES"

Order No. 1208-PM-62-93-93 (4912)

Date of Contract: May 1, 1962

Amount of Contract: \$34,791.00

Contract Number: DA-36-039-SC-89106

Report Prepared By:

L. E. Stone

Geo. N. Webb

Edited By:

J. R. Musgrave

**The Eagle-Picher Company,
Research Laboratories,
Miami, Oklahoma.**

The work performed under this contract was made possible by the support of the United States Signal Research and Development Agency, Fort Monmouth, N. J.

TABLE OF CONTENTS

	<u>PAGE</u>
I. PURPOSE,	1
II. ABSTRACT,.	3
III. PUBLICATIONS, CONFERENCES AND REPORTS,	4
IV. FACTUAL DATA:	
Introduction,.	6
Approach to the Problem,	8
Fabrication,	11
General,	11
Wafer Preparation,	12
Contacting,.	14
Testing Procedures,.	18
Phosphorus Diffusion,.	19
Zinc Diffusion,.	28
Diode Characteristics,	36
Spectral Response,	38
Photovoltaic Studies and Evaluation,	42
Temperature Performance,	45
Ruggedness,.	46
Gallium Phosphide Synthesis,	47
EPITAXIAL GROWTH:	
Ga ₂ O ₃ - Phosphorus Method,	53
Iodine Transport Method,	56
Device Parameters,	59
Discussion,.	61
Electroluminescence,	63
V. SUMMARY,	66
VI. REFERENCES,.	68
VII. PERSONNEL,	69

--*****--

LIST OF TABLES AND ILLUSTRATIONS

	<u>PAGE</u>
Figure 1. Band Gap Energy Versus Depth of Variable Gap Structure, . . .	6
Table I. Cell Fabrication Steps and Sequence,	11
Figure 2. Sub-Surface Damage of Diamond Polished Surface,	13
Figure 3. Chemical Polishing Device,	13
Figure 4. Chemically Polished Gallium Arsenide Surfaces,	14
Figure 5. Diode Characteristics of Typical Devices,	15
Figure 6. Dark Diode Characteristics of Variable Gap Mesa Diode, . . .	16
Table II. Spectral Emission Analysis of Phosphorus,	19
Table III. Variable Gap Cross Section Geometry Specimens,	21
Figure 7. Specimen E-8, GaAs Control, 400x,	23
Figure 8. Specimen #444 - Single Gap Structure, 400x,	23
Figure 9. Specimen #431 - Shallow Variable Gap Structure, 400x, . . .	23
Figure 10. Specimen E-9 - Deep Variable Gap Structure, 400x,	25
Figure 11. Specimen E-10 - Deep Variable Gap Structure, 400x,	25
Figure 12. Specimen #428 - Deep Variable Gap Structure, 600x,	25
Figure 13. Specimen E-5 - Deep Variable Gap Structure, 400x,	25
Table IV. Spectral Emission Analysis of Phosphorus Impurities,	26
Figure 14. Cross Section Variable Gap Device, #503,	27
Figure 15. Surface Resistivity as a Function of Zinc Diffusion,	30
Figure 16. Carrier Concentration as a Function of Zinc Diffusion, . . .	31
Figure 17. Surface Resistivity as a Function of 500°C Zinc Dif- fusion Time,	32
Figure 18. Carrier Concentration as a Function of 500°C Zinc Dif- fusion Time,	33
Figure 19. Induction Heating System for Zinc Diffusion,	34

(CONTINUED ON NEXT PAGE)

LIST OF TABLES AND ILLUSTRATIONS (Con't)

	<u>PAGE</u>
Figure 20. Wafer Positioning for Induction Zinc Diffusion,	35
Figure 21. Diode Characteristics of Deep Variable Gap Device,.	36
Figure 22. Spectral Response of Selected Devices,.	39
Figure 23. Spectral Response - Deep Variable Gap #503,	41
Table V. Photovoltaic Data - Single Gap Devices,	42
Table VI. Photovoltaic Data - Shallow Variable Gap Devices,	43
Table VII. Photovoltaic Data - Deep Variable Gap Devices,.	44
Figure 24. Open-Flow Gallium Phosphide Synthesis System,	48
Figure 25. Gallium Phosphide Synthesis Product,.	49
Figure 26. Epitaxial Growth System, Ga ₂ O ₃ and Phosphorus,.	54
Figure 27. Laue Pattern of Epitaxial Surface,.	55
Figure 28. Iodine Transport Epitaxy System,.	57
Figure 29. Epitaxial GaP Layer on GaAs by Iodine Transport Method, .	58
Table VIII. Epitaxial Device Photo Parameters,.	59
Figure 30. Epitaxial Device Diode Characteristics,	60
Figure 31. Epitaxial Device Spectral Response,	60
Table IX. Fabrication Steps and Sequence for Electroluminescent Diodes,	63

-*****-

I. PURPOSE

The general objective of this work was to investigate the variable band gap structure $\text{GaAs}_x\text{-GaP}_{(1-x)}$, having a gallium phosphide surface concentration approaching 100 percent, decreasing in concentration with depth to a position at which the composition was entirely GaAs. This structure represents a gradient in band gap energy from that of GaP (2.4 e.v.) to that of GaAs (1.35 e.v.). The structure was to incorporate a single p-n junction. The photovoltaic cell diode was considered the best form for evaluation, yielding additional information as to lifetimes, diffusing lengths, etc.

Practical objectives included the establishment of optimums of diffusion, doping, contacting, junction depths and processing techniques to produce efficient devices of this structure. Inherently this implied the minimizing of sheet resistance, preservation of lifetimes and mobilities, and optimizing contacts for ohmicity and low resistance.

Evaluation was planned to define the above mentioned parameters, and to demonstrate any advantageous characteristics such as temperature performance, collection efficiency, spectral response, radiation resistance, etc. It was not considered that solar cell efficiency per se should be a criterion; thus sophistications such as etching, anti-reflectant coatings, grid-
ed contacts, etc., were specifically excluded.

For the purpose of comparison, it was considered useful to attempt

growth of crystals of GaP. Specimens of GaP were to be used for the determination of bulk electronic parameters, contacting, etc., and for epitaxial growth of layers on GaAs. This pursuit was planned to allow comparison of the gradient versus abrupt change in band gap.

This phase was planned as a secondary parallel objective, not to detract from the primary objectives of this investigation.

II. ABSTRACT

Fabrication and evaluation of variable energy gap structures of two categories was carried out; "shallow" devices with 1 to 3 microns of surface GaP, and "deep" devices of 6 to 40 microns depth. Conventional GaAs units were fabricated and evaluated for comparison purposes. Shallow variable gap devices exhibited essentially equal photovoltaic properties as single gap conventional devices, and demonstrate advantages in ruggedness, spectral response, and a numerically small temperature performance.

Initial deep variable gap structures indicated severe compensation from diffusion of impurities during the phosphorus diffusion. Source of these impurities was determined by spectral emission analysis to be the phosphorus. Recent devices fabricated with high purity phosphorus produced competitive, although lower, photovoltaic properties. Significant spectral response differences were observed in these devices. Principal difficulty in realizing the optimum performance is the placement of the junction within the upper GaP, instead of coincident or below the GaP-GaAs transition area. Informative zinc diffusion studies and data are presented. A proposed method of quick, high temperature zinc diffusion is discussed. Surface preparation, contacting techniques and processes are detailed. Evaluation of diode characteristics, spectral response, photovoltaic properties and temperature performance is reported.

GaP synthesis by two methods was achieved and described. Epitaxial growth of GaP on GaAs substrates, carried out for comparison purposes, is described and illustrated. Photovoltaic and diode parameters of epitaxially grown p-on-n junctions are described. Electro-luminescence of variable gap structures were observed and discussed.

III. CONFERENCES, PUBLICATIONS AND REPORTS

Conferences:

The Annual Power Sources Conference at Atlantic City, N.J., May 21, 22, 23, 1962 was attended by Messrs. Louis E. Stone and George N. Webb of this Laboratory. A conference was held at Evans Laboratory, Fort Monmouth, N.J., on May 24th., 1962, with Messrs. Lawrence Schwartz and Joe Mandelkorn. Sample Devices #380, #396, #421, #427 and GaP material sample M6204-AB were delivered to Mr. Schwartz.

A conference was held at the Eagle-Picher Research Laboratories on September 25, 1962, with Mr. Phillip Newman of Fort Monmouth, New Jersey.

The I.R.E.-P.G.E.D. Meeting at Washington, D.C., October 27-29, 1962 was attended by Dr. Jno. R. Musgrave and Mr. Louis E. Stone of this Laboratory. At this meeting a conference was arranged with Mr. Phillip Newman; sample specimens M6210-CD and M6210-CR were delivered.

A conference was held at Fort Monmouth, N.J., on February 13, 1963 by Mr. Louis E. Stone of Eagle-Picher, and Messrs. Robert Yatsko, Phillip Newman, and J.S. Kasperis of Fort Monmouth.

Publications:

An article, "Conversion of Gallium Arsenide to Gallium Phosphide by Solid State Diffusion" was published in the Journal of Applied Physics, September, 1962, issue.

A paper - "Variable Energy Gap Devices" was presented at the I.E.E.E.-A.I.A.A. Photovoltaic Specialists Conference, Washington, D.C. April 10, 1963.

Reports:

Monthly Letter-Type Reports, Nos. 1 to 12, inclusive, were submitted as scheduled.

The First Quarterly Technical Report was distributed August 31, 1962.

The Second Quarterly Technical Report was distributed Nov. 30, 1962.

The Third Quarterly Technical Report was distributed Feb. 28, 1963.

IV. FACTUAL DATA

INTRODUCTION:

The subject of this investigation is the $\text{GaAs}_x\text{-GaP}_{(1-x)}$ system. The specific geometry contemplates a surface layer of essentially 100 percent GaP; the concentration decreases with depth to a distance at which the GaP concentration is zero. Figure 1 illustrates graphically the concentration (or band gap energy) as a function of distance below the surface of the variable energy gap structure.

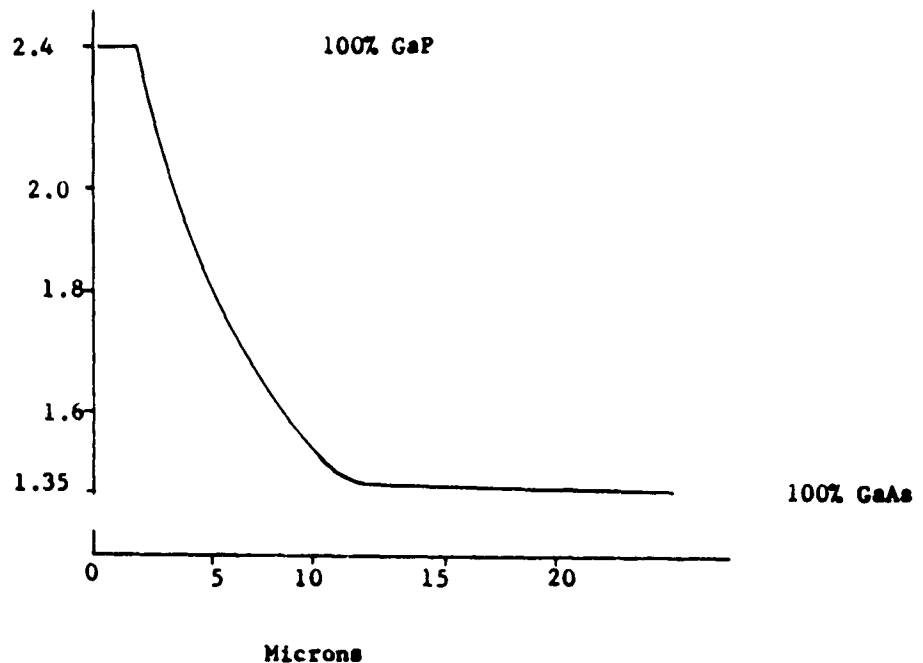


Figure 1. Band Gap Energy Versus Depth of Variable Gap Structure.

This model considers the placing of a p-n junction at any selected depth below the surface.

The theoretical basis for the investigation of this system and geometry is detailed in a previous report⁽³⁾. Stated briefly, the higher energy gap material should result in a higher ratio of photon generated current (I_g) to thermally generated currents (I_o). The higher energy gap material should transmit a larger percentage of photons to a position closer to a deep junction, thereby increasing collection efficiency. The greater latitude in junction depths would allow a thicker, more conductive layer above the junction, decreasing sheet resistance, and increasing radiation resistance. In summary, the graded or variable energy gap structure theoretically should produce increased injection and collection efficiencies, higher I_g to I_o ratio, and better high temperature performance.^(1,2,3) In the field of electro-luminescent diodes, beam-of-light transistors and injection lasers, the higher band gap energies offer promise of improved emission, emission at wavelengths in the visible range, higher injection and collection efficiencies.^(4,5)

The variable band gap structure is achieved by solid state diffusion.⁽⁶⁾ GaP layers approaching 100 percent concentration, with good control in thickness up to 40-microns or more have been produced. Initial device fabrication and evaluation defined one of the major problems which hampered the investigation, namely, the compensation, or conversion to "p" type conductivity, of parent bulk material during the conversion of deep layers of GaP. The source of contamination proved to be the phosphorus and during the last month of work, several deep variable gap structures were produced. More detailed discussion of this phase is made subsequently.

For comparison purposes, epitaxial GaP on GaAs structures were considered, to compare the abrupt versus smoothly graded band gap geometries.

To this end, GaP synthesis was carried out, and several melt-grown ingots of GaP were prepared. Epitaxial layers were grown from this material in the latter part of the contract period and are reported herein. The synthesis, melt growth of GaP ingots, and the epitaxial growth of high quality layers were each significant tasks, beset with many problems. The work on these phases has been particularly fruitful, considering the limited time and effort.

Approach to the Problem:

The fabrication of the structure was undertaken in two general categories, i.e., shallow GaP layers of the order of a few microns, and deep layers of the order of 10 to 20 microns. These two forms were considered to bracket the probable applications and from previous experience, would define one of the most serious difficulties encountered, that of compensation during phosphorus diffusion.

Studies were planned and carried out to define the following:

1. Optimum surface preparation.
2. Optimum phosphorus diffusion schedules and techniques for producing the structure.
3. Optimum zinc diffusion schedules to produce an abrupt, highly doped "p" junction within the GaP layer.
4. Sheet resistance of the diffused layers.
5. Optimum contacting of the "p" and "n" surfaces.
6. The existence and elimination of the compensation, or barrier layer observed in the deep structures.
7. Evaluation of the appropriate electronic parameters and characteristics of diode structure.

The evaluation of the structure was anticipated to be a difficult problem. The state of the art in both materials was - and is yet - not advanced; the difficulty in placing a junction near the surface in the zone of highly concentrated GaP was known. The effect of residual GaAs content in the area

of the junction could be expected to shade or blend any clear cut contrasts in parameters. The device form which would be most sensitive to differences in structure, band gap, etc., was considered to be the photovoltaic cell, and this form was selected.

Several considerations in initial guide-lines were made. The inherent purpose and goal of a deep junction geometry (of at least 2-microns) as compared to conventional GaAs photovoltaic devices, in which very shallow junctions (less than 1-micron) are obtained by etching techniques, ruled out the feasibility of chemical etching - other than for surface cleaning. Photovoltaic efficiency, per se, was not a goal, since this would introduce the added complexities of grided contacts, anti-reflectant coatings, etc., and dilute the central purpose.

Fabrication of photovoltaic devices of the shallow depth category was planned to investigate the problems and techniques of junction formation. These studies were aimed at producing a p-n junction within the GaP layer rather than below it; at evaluating the highest possible zinc carrier concentration consistent with this shallow diffusion; and the determination of diffusion schedules, techniques, and resultant sheet resistances.

Fabrication of the deep variety of photovoltaic structures were planned to discover and eliminate the cause of the compensation problem. Studies were planned and carried out with and without excess arsenic present to explore the possibility of dissociation of the GaAs. Studies of GaAs bulk purity and resistivity were planned and carried out. Rigorous analysis of reactants, processing chemicals and bulk phosphorus were carried out. These studies resulted in successful fabrication of deep GaP layers without compensation effects.

For comparison purposes, fabrication of single gap or conventional GaAs devices were planned and carried out. In these studies, chemical etching was planned only as a corroborative method of measuring junction depths; the same restrictions as to grided contacts and coatings were observed as in the variable gap case.

Concurrently with the central approach, it appeared informative to produce some bulk ingots of GaP. The object of this undertaking was two-fold: To allow comparison of the variable gap structure with its abrupt counterpart, grown epitaxially, and to allow primary determinations as to contact ohmicity, bulk resistivity, transmittance, etc. This effort was planned as an effective way to utilize "dead time", i.e., periods of furnace heat-up and cool down, mechanical and chemical polishing intervals, etc. Studies and techniques of synthesis and melt growth were planned and carried out thus, without penalty to the major effort. In similar fashion some epitaxy of GaP on GaAs was planned and executed.

Evaluation of the devices was planned and carried out to define the appropriate parameters. These included the following:

Bulk Material	- Resistivity - Mobility - Purity
Contacts	- Ohmicity - Resistance
Photovoltaic	- Open Circuit Voltage - Short Circuit Current per unit area - Effective matching (load) resistance per unit area - Conversion Efficiency - Spectral Response - Diode Characteristics
Electroluminescence	- Diode Geometry - Emission Intensity (Relative)

Fabrication:

General.

The fabrication process for photovoltaic devices has been described in detail in previous reports^(7,8,9). Some detailed discussion of the fabrication of other forms will be made subsequently. For the photovoltaic form of the variable energy gap devices the essential fabrication steps for both single gap and variable gap structures are outlined in Table I.

TABLE I
Cell Fabrication Steps and Sequence.

	<u>Variable Gap</u>	<u>Single Gap</u>
1. Dice material to appropriate size,	X	X
2. Lap with 600-Grit Compound to clean saw debris,	X	X
3. Diamond polish to optical finish,	X	X
4. Chemically polish in $\text{H}_2\text{SO}_4\text{-H}_2\text{O}_2\text{-H}_2\text{O}$ etchant,	X	X
5. Rinse thoroughly in deionized water and dry,	X	X
6. Seal in evacuated, purged ampoule with appropriate phosphorus charge and diffuse,	X	
7. Clean chemically in HF or HI acid, rinse, dry,	X	
8. Diffuse zinc to form junction,	X	X
9. Mask surface with Krylon, lap bottom surface, heavily,	X	X
10. Electro-plate nickel on bottom surface,	X	X
11. Lap edges heavily, dissolve Krylon, clean, rinse, and dry,	X	X
12. Mask top surface, sputter platinum collector on top,	X	X
13. Apply solder coating to top and bottom contacts,	X	X
14. Cell ready for evaluation.		

Wafer Preparation:

Some discussion of surface preparation is in order. The diamond polishing of wafers has regularly been used to produce a flat, highly polished surface. Etching of such surfaces has indicated high densities of dislocations, and made attractive a chemical polishing step to remove such damaged layers, while retaining the flat, polished surface. A satisfactory procedure was developed by adapting the technique described by Sullivan & Pompliano⁽¹⁰⁾. Wafers are randomly rotated in a solution of 70 percent H_2SO_4 , 15 percent H_2O_2 (30%), and 15 percent H_2O for periods of about 30 minutes. The resulting surfaces are undamaged, clean and flat. This procedure has improved the reproducibility of the diffusion process significantly.

Figure 2 illustrates the sub-surface damage of a diamond polished GaAs wafer. The wafer was polished optically flat and reflective, using a mechanical DP-Polisher, and very fine grit diamond paste. Subsequent to diffusion, disturbing irregularities in the diffusion front (or junction), which should be planar, were noted. Microscopically these irregularities were related to lines of dislocations at the original surface. To illustrate this effect, a typical flat wafer was partially immersed in the chemical polishing solution mentioned above for 30 seconds. The damage and dislocations are easily visible to the eye, although the un-etched remainder of the wafer appears perfect, when under high magnification. This damage may be observed up to 10 or 20 microns deep.



Figure 2. Sub-Surface Damage of Diamond Polished Surface.

Chemical polishing is done with the previously mentioned solution in device illustrated in Figure 3.

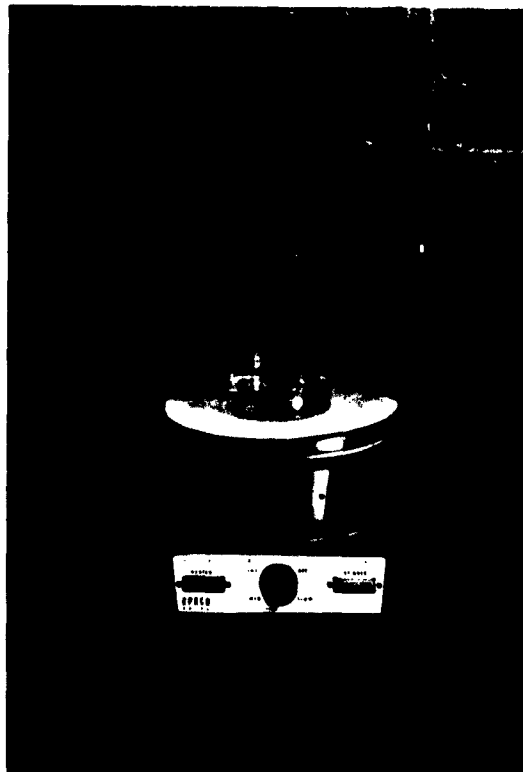


Figure 3. Chemical Polishing Device.

The chemical polishing technique results in a clean, undamaged surface well suited for diffusion. The surfaces are not perfectly flat; gentle shallow undulations can be measured microscopically. Typical appearance is illustrated in Figure 4.



Figure 4. Chemically Polished Gallium Arsenide Surfaces.

Contacting: (Photovoltaic-planar devices)

Electroplated nickel contact is made to the bottom (n) material. It is plated at a rate of approximately 25 ma/cm^2 from the hydroxide (basic) solution usually used for electroless plating.

Sputtered platinum collector contact is made to the top surface, as a 1-mm stripe lengthwise of the wafer.

Both contacts when applied, show slight non-ohmicity and some series resistance. Coating with 60-40 solder eliminates both, and produces a

good contact, as indicated by diode characteristics. Figure 5 illustrates the diode characteristics of single gap and variable gap devices. The two variable gap curves represent the spread of diode forward characteristics: #428 indicates some resistive slope; that of #442 closely approximates the ideal steep characteristic. Both types show the "soft" reverse characteristic of photovoltaic diodes, but confirm the low contact resistance.

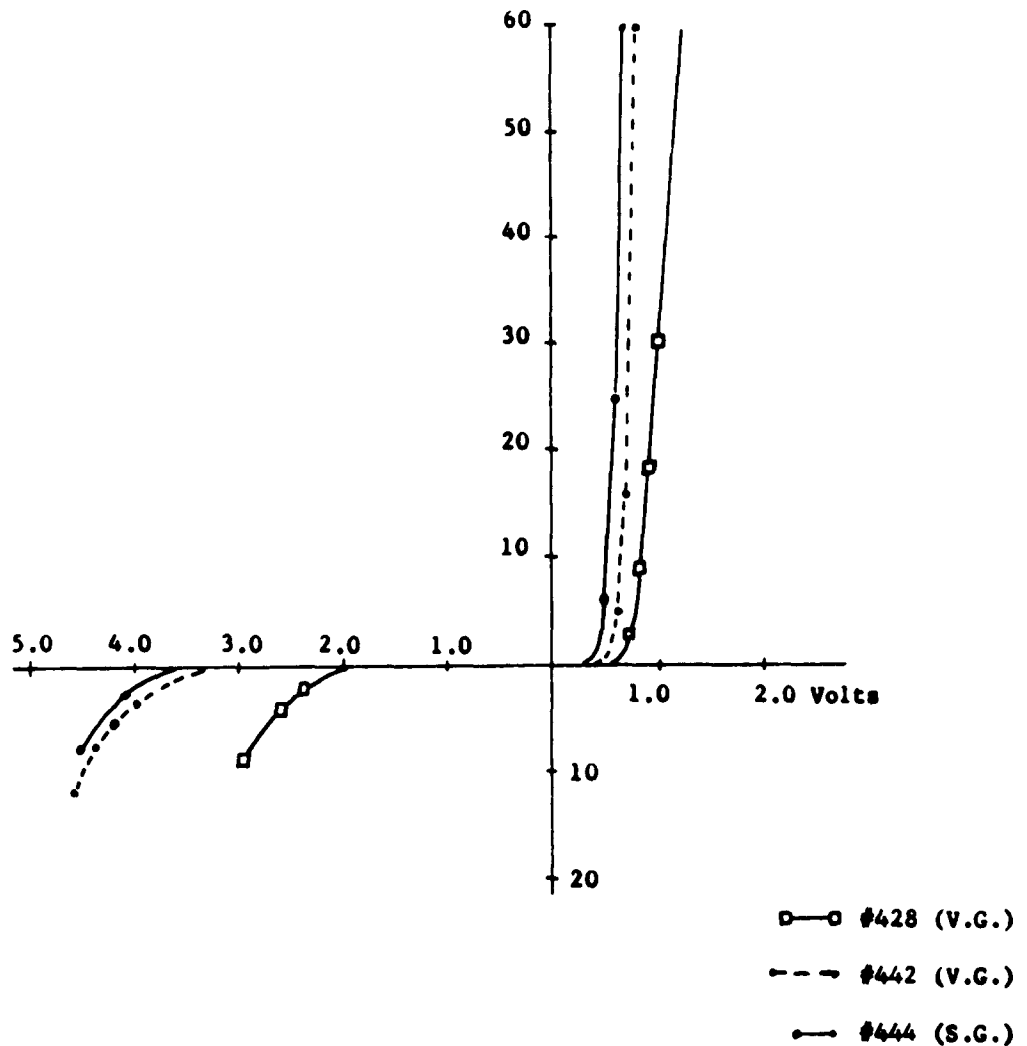


Figure 5. Diode Characteristics of Typical Devices.

Contacting. (Mesa Diodes)

Studies of injection luminescence allowed deeper, more heavily doped junctions. Variable gap structures were contacted by plated nickel on the bottom and in a dot pattern on the top surface, followed by solder coating. The low contact resistance is indicated in the dark diode characteristics of Figure 6.

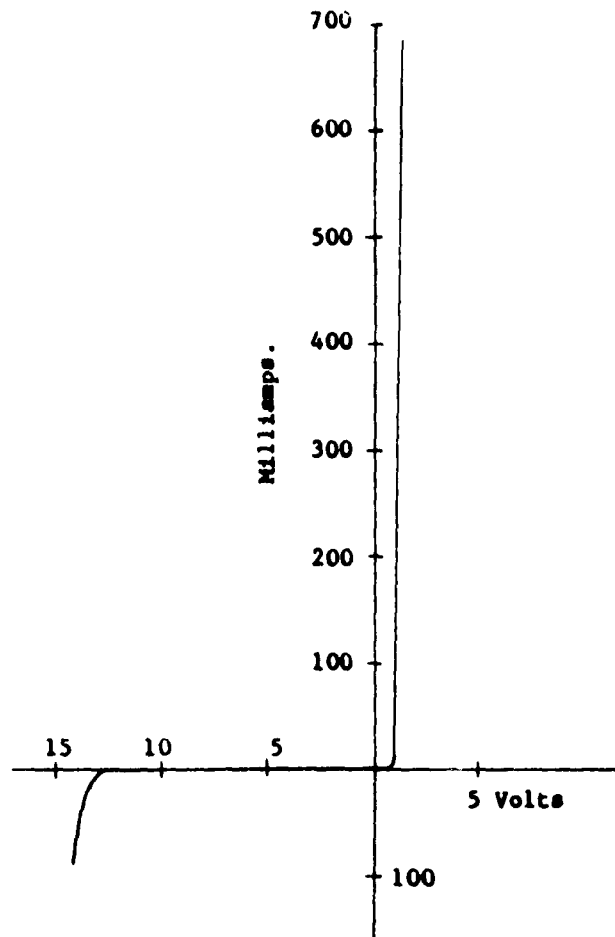


Figure 6. Dark Diode Characteristics Mesa Diode. ELDV-2.

Contacting. (Bulk Gallium Phosphide)

Contacts to bulk gallium phosphide were investigated. Indium contacts applied ultrasonically were adherent, but observed to be non-ohmic. Diode characteristics indicated a symmetrical, double junction on n-type gallium phosphide or low net carrier concentration. Symmetrical breakdown voltages of approximately 5 volts were observed.

Similar bulk material was contacted ohmically by ultrasonic application of lead-indium containing tin or antimony. P-type surfaces were contacted ohmically by ultrasonic application of lead-cadmium or lead-zinc alloy. Typically, the forward break occurs at approximately 1-volt, and some resistive slope was observed. The number of diodes fabricated was statistically small.

High temperature contacts were made by alloying gold-indium to p-type material at 600°C. N-type surfaces were contacted by alloyed gold-tin or lead (previously applied ultrasonically).

Testing Techniques and Procedures:

Testing techniques and procedures are standard and current with the present state of the art, and designed to correlate with other laboratories to the closest practical degree. The following outlines the methods used.

- (a). Resistivity is measured using four terminal, potentiometric method, with current contacts isolated and widely spaced from voltage drop terminals.
- (b). Four-probe resistivity of surfaces is done using conventional 4-probe head and technique.
- (c). Two-probe resistivity or resistance per square measurements are made on cell surfaces using special semi-blunt points to prevent surface puncture.
- (d). Photo-parameters are measured using a Hewlett-Packard Model #425 Micro-Micro Ammeter. I_{sc} is measured as the voltage drop across a precision 1-ohm resistor.
- (e). Light measurements are made in sunlight using an Eppley Pyroheliometer, collimated against reflected light. When laboratory testing is required, a similar calibrated cell is used to adjust an RFL-2 light to give equal I_{sc} current through a 1-inch water filter.
- (f). Spectral response is measured with a Bausch & Lomb Spectrophotometer of the grating type.
- (g). Temperature performance is measured in a special Blue-M regulated oven, with built-in instrument wiring, capable of close, automatic regulation to over 200°C.
- (h). Diode characteristics are measured using the curve-tracer technique, and a Tektronix Model #535 Oscilloscope.
- (i). Cross section device geometry is done using an electro-etch-stain technique developed in our laboratory, in conjunction with a Unitron Microscope fitted with built-in camera.

The subsequent discussion is arranged for logic and continuity, rather than chronologically.

Phosphorus Diffusion:

Red phosphorus, semiconductor grade, from the American Agricultural Chemical Company was used. Wide variations in impurity concentrations were found from batch to batch by spectrographic analysis. Table II illustrates spectro-analyses of the two extremes.

TABLE II

Spectro-Analysis of Phosphorus Lots - Parts Per Million.

	<u>Si</u>	<u>Pb</u>	<u>Mg</u>	<u>Fe</u>	<u>Al</u>	<u>Cu</u>	<u>Ca</u>	<u>Sn</u>	<u>Ni</u>
M6207-BQ	40.0	1.0	5.0	1.0	5.0	1.0	1.0	----	----
M6206-CH	500.0	51.0	30.0	10.0	10.0	2.0	10.0	30.0	5.0

Attempts were made to further purify Lot M6207-BQ by multiple sublimation. Spectro-analysis indicated little or no improvement. Hence selected best grade material was used without further treatment. The impurity levels involved here were considered the major difficulty in fabricating high efficiency deep variable gap structures. Phosphorus diffusion was carried out in evacuated, heavy-wall quartz ampoules. The phosphorus charge, calculated as P_4 , to produce the selected pressure at the desired diffusion temperatures was placed at one end of the ampoule, the specimen wafers at the center, and after five cycles of evacuation-purging with an inert gas, the ampoule sealed off under approximately 1-micron vacuum. After diffusion, the ampoules were moved to the end of the hot zone, and the phosphorus deposited at one end by selective cooling. This end was sawed off in opening the ampoules.

Diffusion schedules were in two general categories, 800°C - 15 atmospheres for periods of one to three hours, and 900°C - 20 atmospheres for periods of two to fifty hours. The former produces "shallow" gallium

phosphide layers of the order of 3-microns thick, the latter "deep" layers of 10 to 20-microns thick, as defined by etch-resistance and staining techniques.

Wafer surfaces regularly were bright and clean, with no erosion, and little, if any, stains or filming. Rinsing with HF was regularly done to remove any possible films prior to zinc diffusion. Cross sections of such variable gap structures, when observed under polarized light at 500x, indicate an homogeneous layer, of orange color, varying in thickness with diffusion schedules.

Photovoltaic devices of the shallow layer geometry exhibited good photovoltaic and diode parameters; the deep layer geometries evidenced poor characteristics. Evidence indicated compensation was occurring; in extreme cases, complete type change was noted in the deep layer geometry.

A study was carried out to define this problem. Specimens of virgin GaAs, zinc diffused GaAs, shallow layer and deep layer variable gap cells were cross sectioned, polished and etch-stained similarly. Microscopic examination and measurement of junctions and layers were made. All specimens were contacted normally, whether a diffused junction existed or not. Table III outlines the results of this study.

TABLE III**Variable Gap Cross Section Geometry Specimens:**

Specimen	Phosphorus History	Zinc History	First Layer Microns	Second Layer Microns	Forward Resistance Ohms	Reverse Resist- ance Ohms
Specimen E-8,	None	None	None	None	350	1700
#444, Single Gap,	None	500°C-3 Hrs.	1.0	None	30	1×10^6
#431, Shallow Variable Gap,	800°C-15 Atm. 1 hour	525°C-1 Hr.	1.0	1.0	25	1×10^6
#E-9, Deep Variable Gap, No Zinc Junction,	900°C-20 Atm. 1 1/2 hours	None	5 to 8	4 to 6	1.5×10^4	1×10^6
#E-10, Deep Variable Gap, Arsenic partial pres- sure, no zinc junction,	900°C-20 Atm. 2 hours	None	4 to 5	6 to 10	7×10^4	1×10^6
#428, Deep Variable Gap, Zinc junction,	900°C- 20 Atm. 2 hours	800°C-3 min.	8 to 10	20.0	----	----
#E-5, Deep Variable Gap, Arsenic partial pres- sure, no zinc junc- tion,	900°C-20 Atm. 2 hours	None	5 to 8	20.0	7×10^6	8×10^6

Referring to Table III, the control specimen did not stain, remaining perfectly clear after twelve minutes, thus assuring that when material is homogeneous, without strata or anomalies of different resistivity or type, no staining occurs as a simple chemical reaction. Three specimens were done; all remained clear, as illustrated in Figure 7. Contact to contact resistance shows the expected small rectification ratio one would expect between large area-small area contacts.

Single Gap Specimen #444, shown in Figure 8, indicates a smooth, 1-micron junction with no secondary staining. (The dark outline of the junction in Figure 8 is photographic shadowing of polishing damage). Resistance measurements indicate the usual rectification ratios found in good diodes.

Variable gap structure, Specimen #431, is of interest as it indicates typical geometry of shallow gallium phosphide devices. Note that a diffused junction is present. Figure 9 illustrates the gallium phosphide layer, about 2-microns thick, and an underlying layer about 1-micron thick. An unsuccessful effort was made to profile the resistance between a micro probe and each of the contacts. Contacting difficulties in the cramped confines of the lens clearance and springing of the probe have thus far prevented accurate measurements. It is interesting that rectification ratios equal, or better, than the single gap structure are obtained. This implies absence of any significant barrier layer in this variable gap device.



Fig. 7. Specimen E-8, Virgin GaAs
Control, No. Layers. (400x)



Fig. 8. Specimen #444, Single Gap
Structure. (400x).

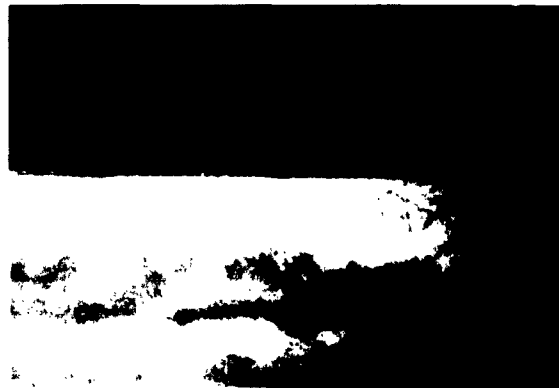


Fig. 9. Specimen #431, Shallow Variable
Gap Structure. (400x).

Variable gap structures formed by phosphorus diffusion at 900°C, 20 atmospheres, for periods of as little as two hours had a gallium phosphide layer on their surface (Figure 10, E-9) and beneath this upper five to eight micron layer, an additional darkly stained band is noted some four to six microns thick. This band is plainly of differing conductivity or type. Note that the contact to contact resistance is also very high in both directions.

Recognizing the possibility that the second layer most easily could be formed by (a) interstitial phosphorus, or (b) depletion of arsenic, a wafer (Figure 11, E-10) was prepared in which the phosphorus diffusion included a partial pressure, (1 atmosphere) of arsenic vapor. As indicated, the second layer was again found, and contact to contact resistance was essentially the same. The only effect observed appeared to be a deterrent to the formation of the gallium phosphide layer, which was thinner. This even might be questioned, and attributed to a variation of phosphorus pressure.

Specimen #428 and Specimen #E-5 directly compare a deep variable gap structure with junction to a phosphorus plus arsenic similar structure. As Figure 12 and Figure 13 indicate, both have similar geometry, including the sub-layer; measurement indicates very similar depths. This supports the contention that a sub-layer is formed, and is the result of the high temperature, high pressure phosphorus step. The junction of the device was accidentally "broken down" in the reverse direction before contact to contact resistance was measured.

This study strongly suggested that compensation and/or type change was occurring along a front preceding the GaP conversion. The probability



Fig. 10. Specimen E-9, Variable Gap Structure. (400x)



Fig. 11. Specimen E-10, Variable Gap Structure. (400x)



Fig.12. Specimen #428, Variable Gap Structure. (600x)



Fig. 13. Specimen E-5, Variable Gap Structure. (400x)

of this being a result of dissociation and loss of arsenic appeared small, as no significant difference was observed in specimens similarly diffused in a partial pressure of arsenic. It was indicated an acceptor impurity in the phosphorus was diffusing into the wafer ahead of the GaP conversion. Thus, while shallow type devices were fabricated successfully, the junctions ultimately were at the bottom of the GaP. In parallel with the shallow layer fabrication and evaluation, effort was made to obtain or purify the red phosphorus in use.

Purification by multiple sublimation was begun, and a program of batch selection of high purity material by spectral emission analysis was carried out simultaneously. Several 30-gram lots of phosphorus were obtained. Spectrographic data on seven such lots are indicated in Table IV.

TABLE IV

Spectrographic Analysis of Phosphorus Impurities.

American Agricultural Chemical Company Phosphorus. (Impurities in PPM)

<u>Ref. No.</u>	<u>Lot No.</u>	<u>Si</u>	<u>Sn</u>	<u>Mg</u>	<u>Fe</u>	<u>Al</u>	<u>Cu</u>	<u>Ca</u>
M6301-CB	Q-002	40.0	5.0	4.0	1.0	5.0	2.0	10.0
M6302-AA	Q-003	N.D.	N.D.	N.D.	N.D.	N.D.	0.5	N.D.
M6302-CB	Q-004	N.D.	N.D.	N.D.	N.D.	N.D.	N.D.	N.D.
M6303-DC	Q-005	20.0	N.D.	2.0	0.5	5.0	1.0	10.0
M6303-BX	Q-006	20.0	N.D.	2.0	0.5	5.0	0.5	6.0

Fisher Micro-Grade Phosphorus.

	<u>As</u>	<u>B</u>	<u>Mn</u>	<u>Mg</u>	<u>Pb</u>	<u>Sn</u>	<u>Si</u>
M6212-BV	50.0	5.0	5.0	50.0	50.0	1.0	5000.0
	<u>Ga</u>	<u>Fe</u>	<u>Al</u>	<u>Cu</u>	<u>Ti</u>	<u>Ca</u>	<u>Cr</u>
M6212-BV	5.0	500.0	500.0	50.0	50.0	5000.0	5.0

The contrast in purity levels indicated in Table IV is emphasized by reference to Table II, of run-of-the-mill phosphorus.

With the acquisition of Q-003 and Q-004 phosphorus, in-house purification effort ceased. Significant improvement was realized in the deep variable gap structure. Compensation was eliminated or reduced to negligible proportions. Several deep variable gap devices were fabricated with improved photovoltaic output, and significant spectral response differences. Figure 14 illustrates the cross section geometry of #503, which has a gallium phosphide layer 7 to 8 microns thick.

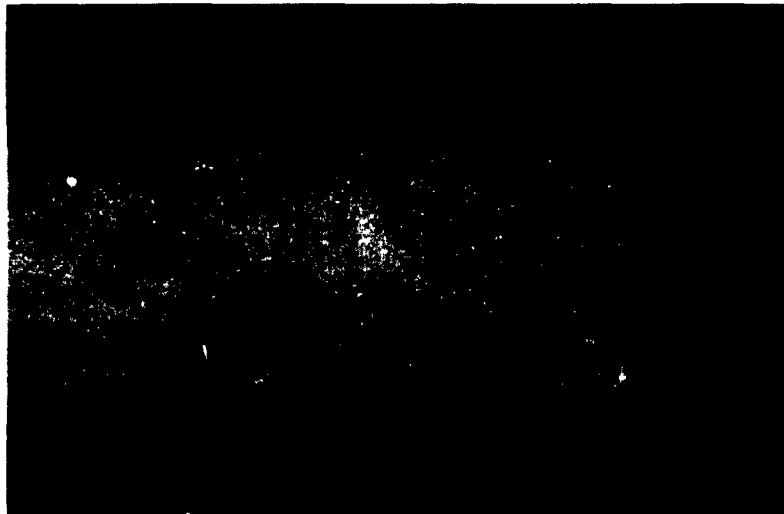


Figure 14. Cross Section Variable Gap Device #503. (400x).

Detailed evaluation will be discussed subsequently. The improvement discussed here occurred at the end of the contractual period, limiting the time available to exploit this breakthrough. It is considered

that further investigation of the deep junction device is certainly warranted.

Zinc Diffusion.

Zinc diffusion is routinely done in fused silica boats, in a reducing (hydrogen) atmosphere. The variable gap and/or single gap wafers are placed centrally, with small pieces of high purity zinc at each end of the boat. The boat is held outside the hot zone of the split-type tube furnace until stabilized at the desired temperature, then moved manually to the exact center of the heated tube, and after the desired diffusion time, moved again to the cool, down-stream end. The tube and boat are removed entirely from the furnace and evaporative water cooling used for rapid cooling. This is done in cognizance of the work by Gershenson, et. al.,⁽¹¹⁾ who advise quench cooling to prevent formation of precipitation site trapping centers. Purging is done with argon; thorough outgassing with moderate flow hydrogen is done before inserting the boat in the hot zone, at which time hydrogen flow is reduced almost to nil; following diffusion, high rate flow is done to sweep zinc vapors out.

An abrupt p-n junction was desired, having high zinc carrier concentration (10^{20} atoms/cc). This goal is contrary to the objective of placing the junction within the gallium phosphide layer. Zinc Diffusion in gallium phosphide is significantly more rapid than in gallium arsenide. Thus a conflict arose in which low temperature would enhance depth control, but prevent good carrier concentrations.

To define the equilibrium concentration obtainable, studies of surface resistivity, ohms per square, as a function of diffusion temperature were carried out on variable gap structures of the shallow variety, for temperatures of 500°C, 550°C, and 600°C. In each case, four to six wafers, including one virgin gallium arsenide control blank, were diffused using identical techniques, for different times at a certain temperature. Many 2-probe measurements of each wafer were made. The scatter of these measurements was very small, of the order of ten percent maximum for a single wafer, and five percent or less between wafers. The average of these measurements are plotted in Figure 15, for 500°C, 550°C, and 600°C, respectively. Subsequently trials were made to check the reproducibility of the technique. In all cases, reproducibility was good, within the measurement scatter, with similar material.

The surface carrier concentrations derived from the surface resistivity are indicated in Figure 16.

The surface carrier concentration is observed to increase with temperature, and equilibrium concentrations approaching $10^{19}/\text{cm}^3$ are attained at 600°C. Typical variable gap cells of 700°C, 15 atmospheres - 2 hours, when zinc diffused 600°C - 10 minutes, exhibit gallium phosphide layer of the order of one to three microns thickness with a p-n junction slightly below the bottom of the gallium phosphide layer. Effort to increase the carrier concentration by extending the zinc diffusion time, moves the junction deeper into the gallium arsenide, with noticeable deterioration of photo parameters.

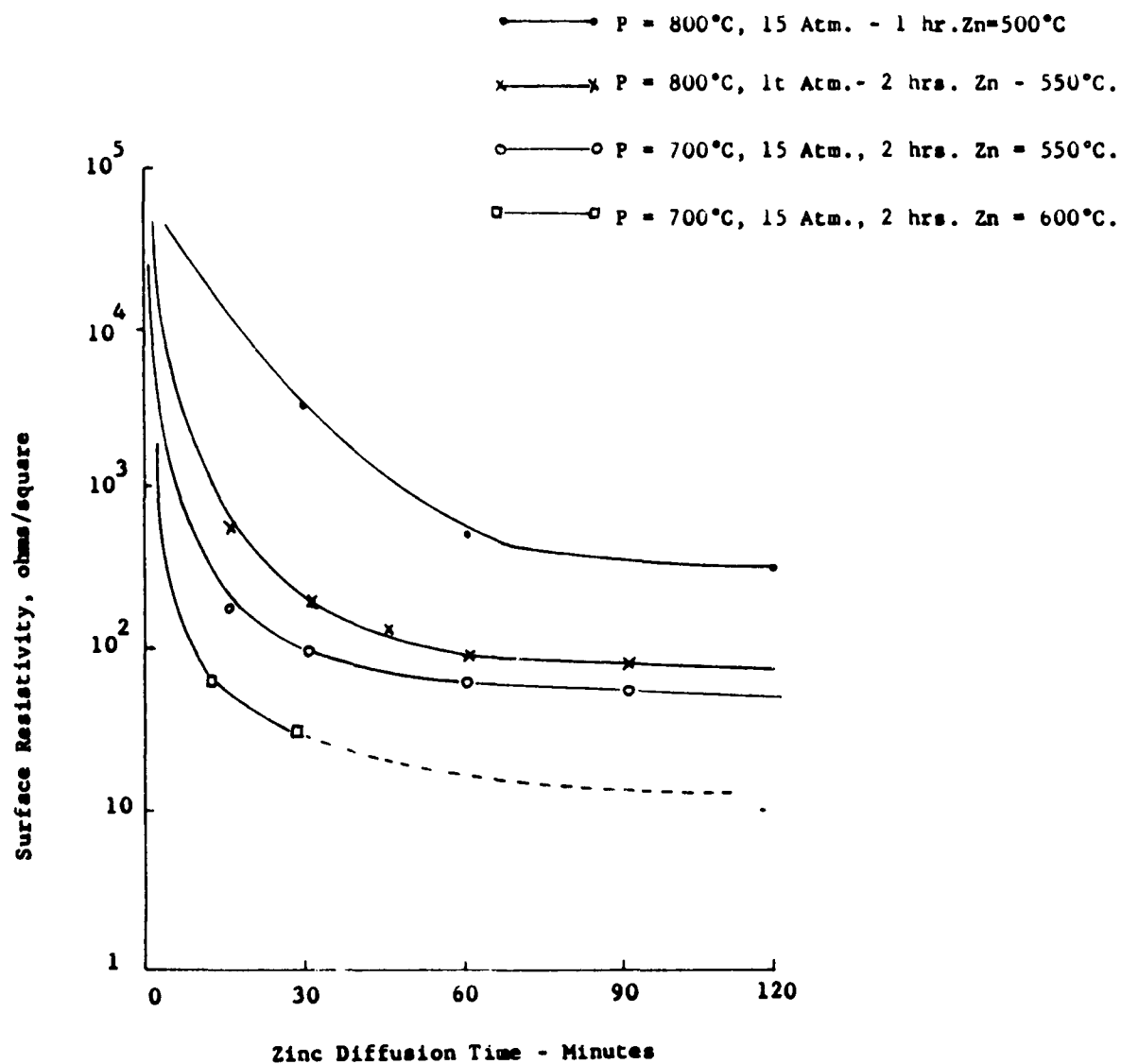


Figure 15. Surface Resistivity as a Function of Zinc Diffusion.

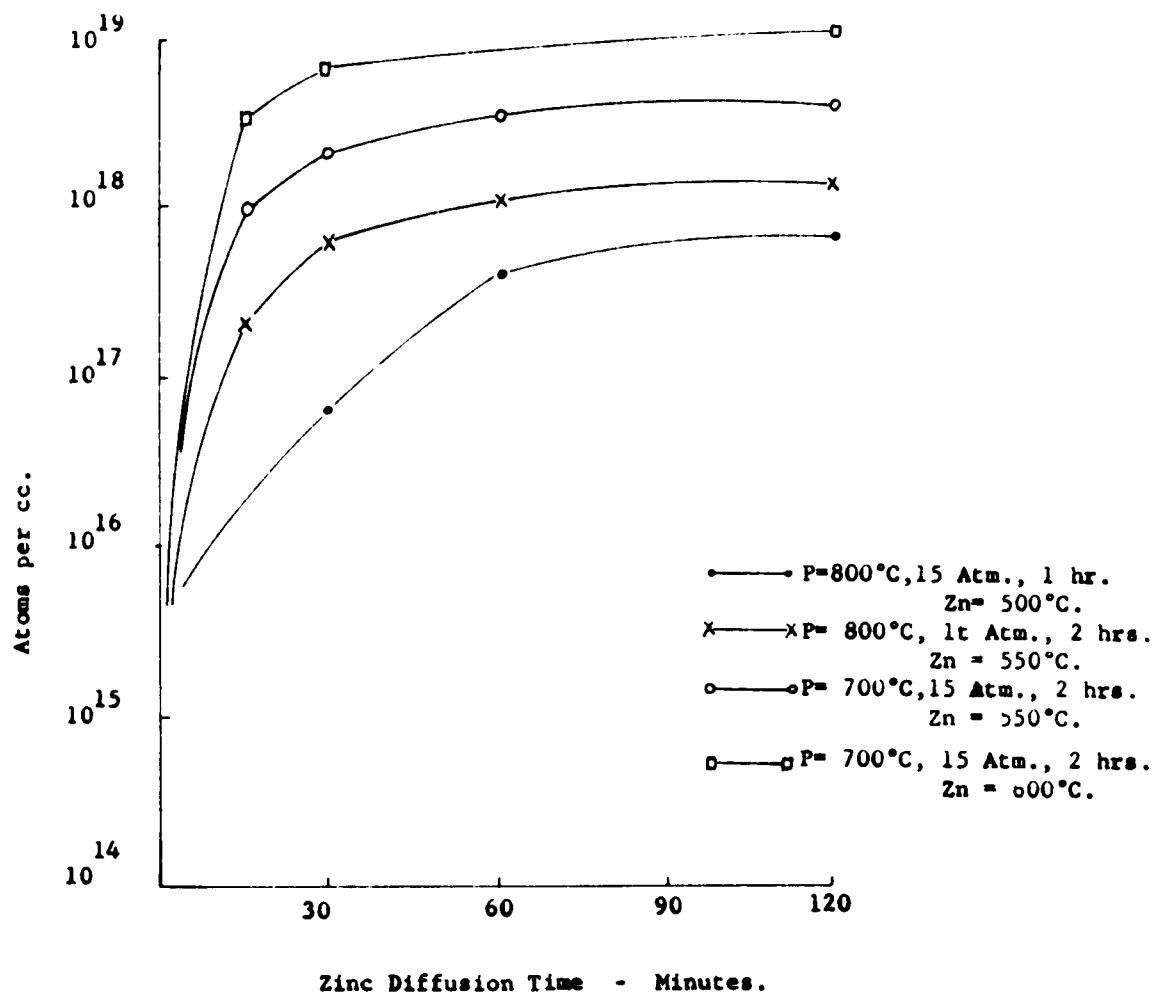


Figure 16. Carrier Concentration as a Function of Zinc Diffusion.

To explore the possibilities of low temperature diffusion fully, for the formation of shallow junctions, a study was carried out in which several shallow variable gap structures were diffused at 500°C for succeeding 30-minute periods, with 2-probe surface measurements made between each period. The 2-probe resistance per square was chosen as it promised less damage to the surface, although admittedly less accurate. Results of this study are illustrated graphically in Figure 17. The surface resistivity levelled off at approximately 300 ohms per square, indicating that excessive sheet resistance would preclude optimum efficiency.

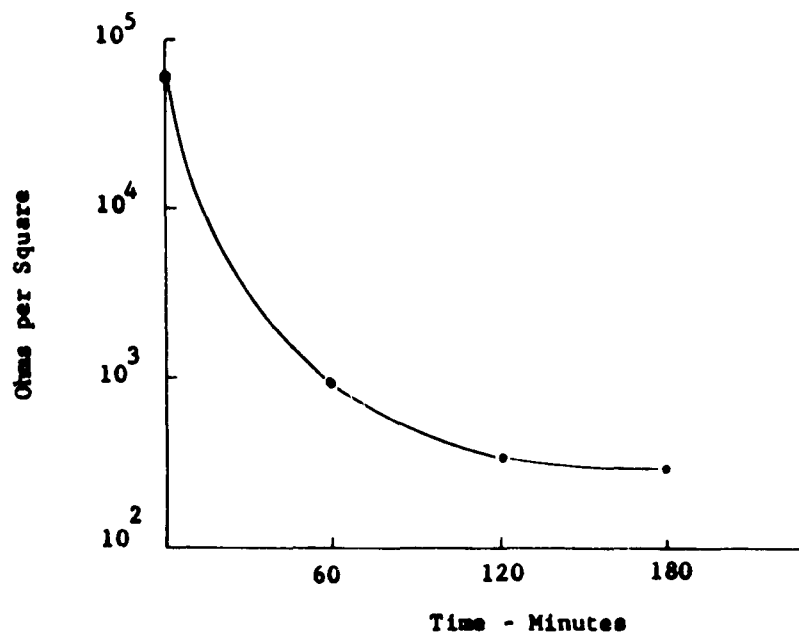


Figure 17. Plot of Surface Per Square Versus Time of Diffusion at 500°C.

The equilibrium concentration, derived from the surface resistivity, is illustrated in Figure 18. As indicated the concentration of approximately 10^{18} atoms/cc was two orders of magnitude low. Thus the use of low temperature (500°C) zinc diffusion, although restricting junction penetration, incurs an intolerable penalty in concentration and precludes the realization of an optimum characteristic junction.

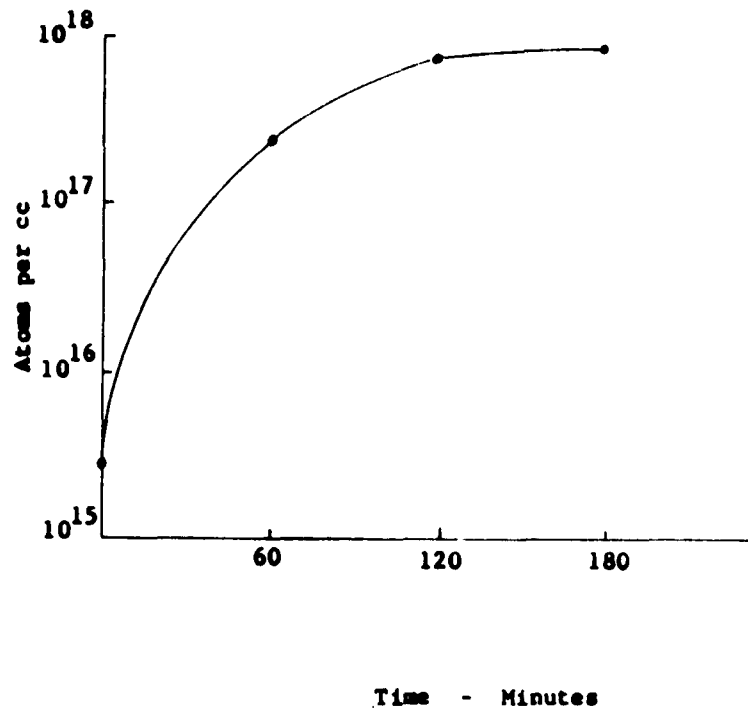


Figure 18. Plot of Surface Carrier Concentration Versus Time of Diffusion at 500°C.

An alternate method of zinc diffusion by induction heating was explored briefly. The advantages of this system were as follows:

- (1). The heating cycle could be very rapid. (to 800°C in a few seconds), with complimentary rapid cooling, thereby allowing close control of short-time diffusion.
- (2). The variable gap wafer was the hottest part of the system; thus no transfer of contaminants would occur from the cool quartz walls to the hot substrate.
- (3). Quick, sharp diffusion steps would allow multiple, incremental penetration steps of junction depth to optimize the device.

A suitable R/F generator was adapted to function at 30 m/cs, to allow coupling to small area wafers. The system is illustrated in Figure 19.

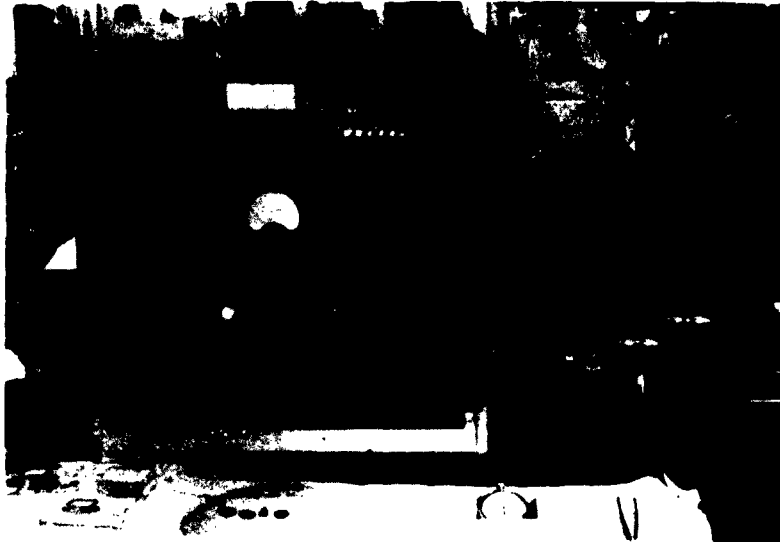


Figure 19. Induction Heating System for Zinc Diffusion.

Figure 20 illustrates the physical placement of the wafer.



Figure 20. Wafer Positioning for Zinc Diffusion by Induction Heating.

The method did realize the advantage in time, temperature and environment. One difficulty arose, in that control of the zinc vapor concentration was difficult. Excess zinc vapor produced alloying and condensation on the wafer surface, and consequently reproducible results were difficult to obtain. It is worth noting that excellent results were obtained in some diffusion runs. Unfortunately, the technique of diffusion from a zinc doped SiO_2 film was not known to us at this time⁽¹²⁾. This method of control of the zinc dopant would provide the final link for excellent junction control.

Diode Characteristics:

Evaluation of diode characteristics was made using the curve tracer technique. Typical diode characteristics are illustrated in Figure 5 of single gap and shallow variable gap structures. Typical diode characteristics of the deep variable gap structure show a measurable difference in forward break, as illustrated in Figure 21.

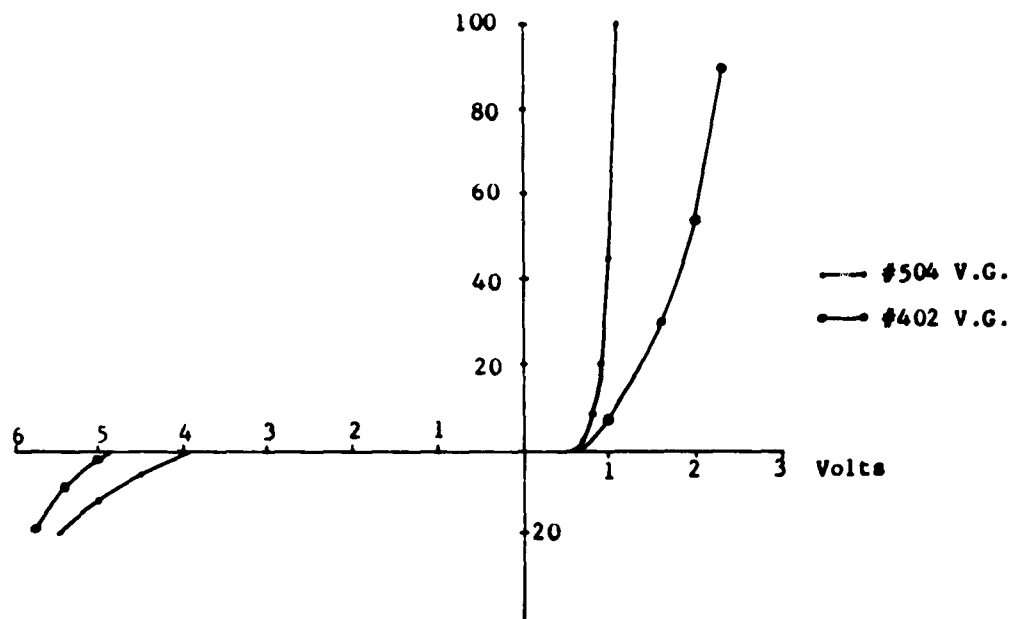


Figure 21. Diode Characteristics of Deep Variable Gap Devices.

The forward break in conductivity in the lately improved deep structure is regularly at 0.8 volts or more, whereas in the other structures conduction first is noted at about 0.6 volts. It could be argued that this difference was a reflection of increased series resistance; such does not appear to be the case. The total series resistance at high values of current, defined by the slope or steepness of the forward characteristic, is obtained as the ratio of change in voltage to change in current; this slope is observed to be essentially the same in the case of the single gap and shallow variable gap cells. It is observed to be 2.5 ohms in both cases, where the shallow junction objective limited carrier concentrations. In the deep variable gap structure, this value was observed to be 1.5 ohms. The decrease is considered the result of increased conductivity in the upper gallium phosphide diffused layer. The increase in forward break voltage is thus not resistive effects, but real. The increase may be attributed to either of two factors; increase in junction gradient in abruptness, or the effect of a significant increase in band gap. Since zinc diffusion schedules, sheet resistivities, etc., were essentially the same, the latter is favored. This is further supported by spectral response data.

Spectral Response:

Spectral response has been used to monitor the improvements in junction depths, collection efficiencies, and evaluation of relative lifetimes and diffusion lengths. The single gap device is observed to peak at approximately 0.8 microns. A sharp abrupt band edge drop is observed at 0.825 microns. In the blue region, response broadens with decreasing junction depth, without shifting the peak response at 0.8 microns. Typical, state-of-the-art response is indicated in Figure 22, by #435.

The shallow variable gap device exhibits a peak at 0.7 microns, increased blue response, and onset of drop in response at 0.750 microns. The increased blue response is characteristic, with junction depths of the order of three microns. Number 431 illustrates typical spectral response of such a device.

The deep variable gap structure exhibits a response characterized by a double peak; the major peak occurring at the band edge energy of gallium arsenide, 0.835 microns, and a separate peak at approximately 0.475 Microns; the band edge energy value of gallium phosphide. A third, small peak is observed at 0.575 microns. The response of such a device, #391, is illustrated also in Figure 20. This particular device had a GaP layer of 30 microns, with a junction at - or slightly above - this depth. The blue response peak is considered evidence of the gallium phosphide contribution to total generated carriers, and that the junction lies slightly above the gallium arsenide interface, in predominantly gallium phosphide.

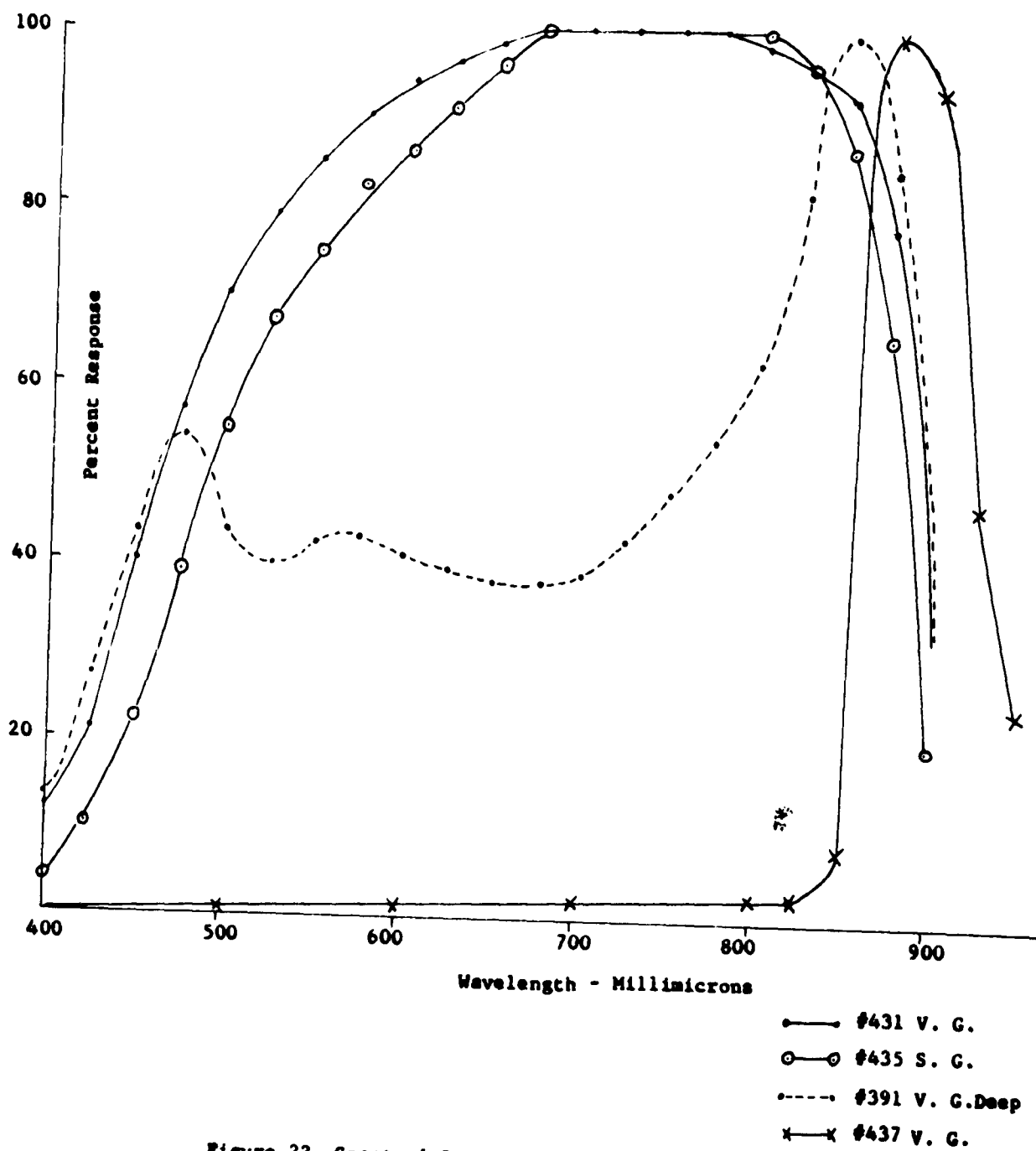


Figure 22. Spectral Response of Selected Devices.

The location of the 0.475 peak, device #391, is observed to approximate the blue response of shallow device #431. It is conceivable that the peak is the result of decreased mid-range response, due to trapping levels from impurity contamination during the phosphorus diffusion. This concept is tenable, since phosphorus contamination was known to be producing some compensation at the time this unit was made. To clarify this question, a similar wafer was diffused with a carefully selected group of the known phosphorus contaminants. This unit, #437, (Figure 22), exhibited a unique response, essentially that of 100 micron band pass, centered at 0.900 microns. The higher energy response is very low, but of a linear increase nature with no indication of peaks or valleys. It appears unlikely therefore that trapping levels can be considered to explain the double peak effect in deep gallium phosphide device #391.

The recent improvement in deep-type devices corroborates this data. Spectral response of #503 illustrated in Figure 23, indicates a definite, broad peak between 0.475 and 0.600 microns. This unit had an 8-micron gallium phosphide layer, with a junction coincident with this 8-micron level. Surface type, resistivity, diode characteristics and microscopy by etch-stain techniques all support the contention that compensation was not involved in the structure of #503. Thus it appears tenable to consider this peak in blue response to be a gallium phosphide contribution of generated carriers.

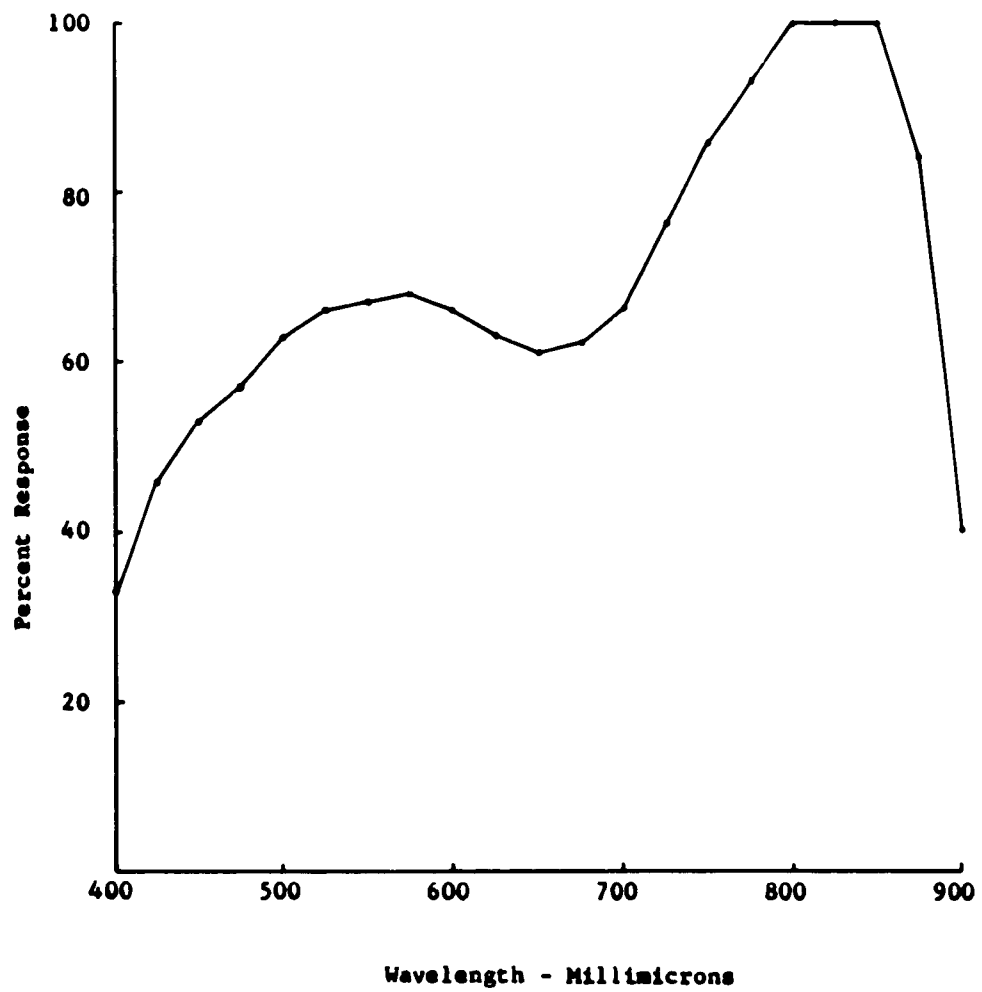


Figure 23. Spectral Response of Deep Variable Gap Device #503.

Photovoltaic Studies and Evaluations:

Approximately 150 finished voltaic devices were fabricated and tested. At least an equal number were made for destructive tests, such as cross section microscopy. Approximately one-fourth of these were single gap structures, for monitor and comparison purposes; one-half were of shallow variable gap structure, and the remaining one-fourth were the deep variable gap type. ("Shallow" refers to units with gallium phosphide layers of the order of one to three microns; "deep" implies five to twenty microns thickness).

In comparing the single gap data, it must be borne in mind that these units were generally fabricated with abruptly doped junctions of the order of 1-micron or less in depth, while the variable gap units junctions were always at least as deep as the gallium phosphide layer. All units had a single collector contact, none were chemically etched or otherwise optimized; no anti-reflectant coatings were used. Table V indicates representative characteristics of single gap devices.

TABLE V

Photovoltaic Data - Single Gap Devices

<u>Identity</u>	<u>V_{oc} Volts</u>	<u>I_{sc} ma/cm²</u>	<u>Eff_{mp} Percent</u>	<u>V_L Volts</u>	<u>Sunlight Intensity - mw</u>
380	0.74	14.0	6.8	0.60	93.0
382	0.72	17.0	7.1	0.54	92.6
403	0.70	14.0	6.1	0.50	92.0
448	0.74	10.8	5.4	0.56	93.1
450	0.75	9.0	5.0	0.60	91.2
462	0.76	15.5	5.0	0.44	91.2
465	0.80	10.5	5.5	0.58	90.3
468	0.80	10.5	5.6	0.62	91.2

NOTE: #380 and #382 fabricated from high mobility material.

Table VI indicates similar data for shallow gap units.

TABLE VI

Photovoltaic Data for Shallow Variable Gap Devices

<u>Identity</u>	<u>V_{oc} Volts</u>	<u>I_{sc} ma/cm²</u>	<u>Eff._{ap} Percent</u>	<u>V_L Volts</u>	<u>Sunlight Intensity - mw</u>
385	0.70	14.7	5.9	0.52	92.0
396	0.70	17.5	6.0	0.46	88.0
405	0.68	17.0	6.0	0.52	91.5
421	0.68	9.5	5.6	0.52	84.0
429	0.72	8.5	4.4	0.56	92.0
431	0.70	9.1	4.5	0.52	87.6
433	0.72	12.0	4.0	0.48	91.0
459	0.69	10.5	4.7	0.52	92.1
466	0.79	12.1	6.4	0.62	92.2
472	0.72	6.8	3.6	0.50	83.0

Variations over the span of the tabulated data are partially the result of excursions in zinc diffusion schedules aimed at compromising shallow junction depths with highest carrier concentration. Unit #466 represents the best approach to this compromise. Diffusion schedules of this unit were phosphorus 800°C - 15 atmospheres, 2 hours; zinc 600°C - 10 minutes.

Deep variable gap structures suffered severely from the previously discussed compensation effects. Photovoltaic parameters were usually very poor; when preliminary measurements (low V_{oc}, I_{sc}, and highly resistive diode characteristics) indicated sub-junction barrier layers or compensation, sunlight efficiency measurements were omitted.

Table VII indicates data obtained on deep variable gap structures which suffered less severe compensation.

TABLE VII

Photovoltaic Data for Deep Variable Gap Devices

<u>Identity</u>	<u>GaP Depth (Microns)</u>	<u>V_{oc} Volts</u>	<u>I_{sc} ma/cm²</u>	<u>Eff_{mp} Percent</u>	<u>V_L Volts</u>	<u>Light Intensity-mw</u>
397	20.0	0.59	2.0	1.0	0.36	90.0
398	18.0	0.69	3.0	1.0	0.40	88.0
401	22.0	0.42	3.5	1.0	0.36	88.0
402	20.0	0.63	3.5	1.0	0.46	90.0
406	20.0	0.27	3.0	1.0	0.22	90.0
503	8.0	0.72	6.0	3.0	0.52	91.0
504	10.0	0.72	7.0	4.0	0.56	55.0

Several considerations must be made in interpreting these data. In the case of the single gap units, higher efficiencies per se could be reported by etching to optimum junction depth, multiple grided contacts, and application of anti-reflectant coatings. It is considered that efficiencies of the order of 10 percent might be obtained in this way. It is reasonable to conjecture that similar improvements might be feasible in the shallow variable gap structures, and at least to some degree in the latest deep structures.

The general comparison of data penalizes the shallow variable gap structures due to the inability to place a junction within the upper part of the gallium phosphide area, thus not realizing the potential benefits thereof. Nevertheless, it appears that the shallow variable gap structures, with junctions of the order of three microns, are capable of equal efficiencies as the conventional GaAs unit. The effect of compensation during the phosphorus diffusion step, in all except the latest deep structures, drastically reduced their photovoltaic properties. In the recent deep structures, where compensation effects were minimized or eliminated, photovoltaic properties are significantly better. This is particularly true of #504; the sunlight test data were made on a day when haze and thin clouds reduced the light to only 55 milliwatts. Normally, sunlight intensity is approximately 90 milliwatts; thus I_{sc}/cm^2 would normally be of the order of 10 to 12 ma/cm², and an increase in Eff_{mp} could be expected.

In summary, no significant advantages in photovoltaic properties were demonstrated; but at least equal performance was observed in the shallow gap units, and the more recent deep structures were approaching this value.

Temperature Characteristics:

Demonstration of an increase in the temperature performance of the variable gap units over the conventional type of gallium arsenide unit was one objective in evaluation. V_{oc} , I_{sc} , and Eff_{mp} were measured over the region 25°C-200°C on several representative specimens of single gap, shallow and deep variable gap units.

The drop in V_{oc} with increasing temperature for single gap units of our own, and for those fabricated elsewhere, gave a straight line slope of 0.00234+ volts/°C. This slope was reproducible.

The drop in V_{oc} of variable gap cells was regularly less, 0.00210 volts/°C. The difference numerically is small, and might be questioned. It is considered real, and quantitatively small due to the inability to place the junctions in an area of predominantly gallium phosphide material.

The I_{sc} versus temperature curves for variable gap units gave a more inclined rise with temperature than the single gap units. Single gap units indicated 25°C/200°C change in I_{sc} of 120 percent; variable gap units indicated 130 percent to 140 percent.

The Eff_{mp} of variable gap units indicated a numerically smaller rate of decline with temperature than the single gap units, the order of difference being similar to that of V_{oc} versus temperature.

In summary, a small advantage in temperature performance was observed in the variable gap structures.

Ruggedness:

The variable gap structures demonstrate a dramatic difference in ruggedness, due to the presence of the gallium phosphide layer. Normal techniques in probing of surfaces, temperature cycling, handling, etc., could be done at will with little fear of damage. Surfaces were relatively immune from damage by normal cleaning etches, deep structures could be successfully nickel plated on the top surface without damage. Qualitatively, the variable gap structures, characterized by this ruggedness, contrasted notably with the damage sensitivity of the single gap units.

Gallium Phosphide Synthesis:

Initial guide-lines of the investigation included the comparison of variable gap, diffused-type structures with step-type structures of gallium phosphide on gallium arsenide, in which little or no grading of the transition region occurs. The course of the investigation reached the point where such comparison would be very useful and informative. Epitaxial growth appeared the logical method of achieving the step-type structure. Tentative efforts at synthesizing gallium phosphide from elemental gallium and phosphorus were successful and ingots, essentially single crystal, were made by synthesis-melt growth in a high pressure system⁽¹³⁾. Subsequent work reported in the literature by Bodi⁽¹⁴⁾ appeared attractive as a method of synthesis, where the end product is not required to be massive single crystal ingots, as is indeed the case here. Thus, gallium phosphide was synthesized in a system modeled after the Bodi method, as source material for epitaxy.

The general synthesis system is illustrated in Figure 24. Phosphorus is sublimed at 400°C in one zone of a multiple-zone furnace, and carried by dry hydrogen gas over a charge of Ga_2O_3 at 900°C in a second zone of the furnace. Hydrogen flow rates are minimal. The exit of the quartz reaction tube is enclosed in a dry ice cold zone to trap vapor reaction products. Exhaust gas is passed through a potassium permanganate trap and exhausted or burned. Reaction time is of the order of several hours. Minimal reaction zone temperatures and hydrogen flow rates encourage the growth of needle structure growth. Figure 25 illustrates the gallium phosphide product. Recovery of gallium as gallium phosphide in the initial runs was approximately 75 percent.

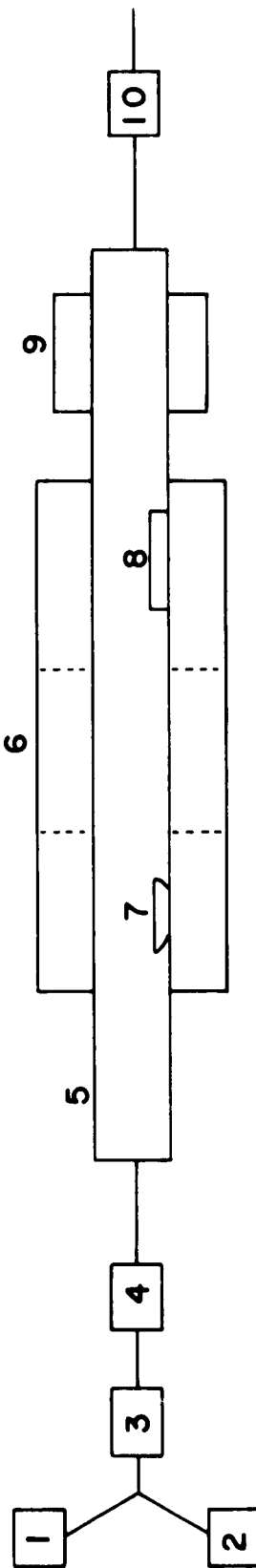


Figure 24. Open-Flow Gallium Phosphide Synthesis System.

- 1. Argon
- 2. Hydrogen
- 3. Acetone - Dry Ice Trap
- 4. Molecular Sieve
- 5. Quartz Tube
- 6. 3-Zone Furnace
- 7. Phosphorus Charge
- 8. Ga_2O_3 Charge
- 9. Dry Ice Condenser
- 10. Bubbler



Figure 25. Gallium Phosphide Synthesized by Open-Flow System.

The surface of the gallium phosphide was a dense growth of large needles, microscopically symmetrical and highly transparent, of yellow-orange color. Beneath the needle was a mat of gallium phosphide powder. Removal of both the needles and mat revealed an adherent coating of gallium phosphide on the fused silica boat. Samples of starting materials, needles, and powder scraped from the boat were analyzed by emission spectroscopy. Impurity data of these specimens are tabulated in Table VIII. The residual powder encrusting the boat was sintered for ten hours at 1000°C and analyzed for impurity content. These data are included.

TABLE VIII

Impurity Analysis of Starting Materials and Synthesized
Gallium Phosphide.

<u>Specimen</u>	<u>Identity</u>	<u>Si</u>	<u>Pb</u>	<u>Fe</u>	<u>Al</u>	<u>Mg</u>	<u>Ca</u>	<u>Cu</u>	<u>Sn</u>	<u>Total PPM</u>
Lot 137-1	Ga ₂ O ₃	-	<0.07	-	-	0.15	0.66	0.34	<0.1	1.32
M6207-BQ	Phosphorus,	40.0	<1.0	1.0	5.0	5.0	1.0	1.0	-	54.00
M6209-BS	Gap Needles,	0.5	<0.1	1.0	0.2	-	1.0	-	-	2.80
M6209-BT	GaP off Boat,	100.0	<0.1	3.0	0.5	-	2.0	-	-	105.60
M6209-BU	Gap off Furnace Tube,	100.0	<0.1	0.5	0.5	-	0.5	-	-	101.60
M6211-AA	Residual GaP Sintered*	5.0	-	-	10.0	3.0	10.0	2.0	-	30.00

NOTE: * = Residual GaP chg. sintered 10 hours, 1000°C in Hydrogen ambient atmosphere.

The data indicate some of the impurities from the Ga₂O₃ and phosphorus is carried over in the gallium phosphide, but especially in the needle growth, an impurity segregation process is evident. High silicon contamination from the fused silica boat is apparent; this may be alleviated by retaining a gallium phosphide covering on the boat.

Specimens of the needles were submitted for x-ray diffractions study⁽¹⁵⁾. The Laue patterns indicated very good single crystal structure with no indication of mixed phases. The diffraction powder study is summarized in the following report.

A single needle-shaped crystal was selected for a single crystal pattern and the remainder was ground for a powder pattern. The results are tabulated and compared with two earlier samples (M6109-AQ and M6204-AB).

The powder pattern of M6209-DM was measured and both the inter-planar spacings (d value) and the edge length of the unit cell (a_q) were calculated. Gallium phosphide has a diamond structure similar to zinc sulfide in the sphalerite form. Since gallium and phosphorus ions have different diffracting properties certain planes give diffraction lines which do not produce lines in a diamond structure comprised of only one kind of atoms. These planes are the (200), (222), (420), (600), and the (622). In several instances these lines are very weak and the inability to measure them does not indicate their absence.

The pattern of the needle-shaped crystals contains a low theta line at about 3.24° which has been observed on previous samples but has not been entirely explained. If arsenic were present it could be accounted for as a second phase, perhaps as a surface layer, of a gallium arsenophosphide solid solution. If arsenic is completely absent two possible explanations can be suggested: The grinding of the sample to a powder was accompanied by a strong odor of "matches" and it is possible that traces of mixed oxide-phosphide account for the extra line. The other possibility is that the mechanical work done in grinding resulted in the crystal being partially converted or "smeared" to an unstable or strained condition which gives rise to this extra line. Opposed to this, however, is the fact that the lines are not broadened.

The unit cell values reported in the literature when compared with

those measured in this laboratory are in reasonably good agreement. However, since the materials with which we are working are perhaps purer than those available to previous investigators the actual values and the differences in results are of interest. The small difference becomes significant when the influence of impurity atoms on unit cell dimensions is considered.

Wyckoff gives a value of 5.436 \AA but the literature reference is not given. The recent publication of Giesecke & Pfister (Acta Crystallographica, 11, 369, (1959) gives a value of 5.4505 \AA which is based on the single (531) plane. Quoted in the G. & P. paper is a 1926 value of 5.447 due to Goldschmidt. Many factors play a part in determining the final values assigned to a unit cell dimension in addition to the sample. Tabulated below are the measured values obtained here on three gallium phosphide samples and data on the determinations and comparisons with literature values:

Sample A_0

M6109-AQ	5.4502	Weighted mean of all lines (Accepted)
M6204-AB	5.4447	Weighted mean of all lines
	5.4508	Weighted mean of doublets (Accepted)
M6209-DM	5.4495	Weighted mean of all lines (Accepted)
	5.4519	Weighted mean of doublets
	5.4466	Refined by a $\sin^2 \theta$ method
Literature:	5.4505	Giesecke and Pfister
	5.447	Goldschmidt
	5.436	Wyckoff

NOTE: It appears that a value of a_0 in the order of $5.4500 \pm 0.005 \text{ \AA}$ is very close to the true value.

Tentative measurements of resistivity of these needles were made. Contacting was by silver paste on copper laminate mounts. This contacting indicates fairly uniform resistivities of approximately $1 \times 10^6 \text{ ohm-cm}$. The resistivities were not greatly sensitive to light.

those measured in this laboratory are in reasonably good agreement. However, since the materials with which we are working are perhaps purer than those available to previous investigators the actual values and the differences in results are of interest. The small difference becomes significant when the influence of impurity atoms on unit cell dimensions is considered.

Wyckoff gives a value of 5.436 \AA but the literature reference is not given. The recent publication of Giesecke & Pfister (*Acta Crystallographica*, 11, 369, (1959) gives a value of 5.4505 \AA which is based on the single (531) plane. Quoted in the G. & P. paper is a 1926 value of 5.447 due to Goldschmidt. Many factors play a part in determining the final values assigned to a unit cell dimension in addition to the sample. Tabulated below are the measured values obtained here on three gallium phosphide samples and data on the determinations and comparisons with literature values:

Sample a_0

M6109-AQ	5.4502	Weighted mean of all lines (Accepted)
M6204-AB	5.4447	Weighted mean of all lines
	5.4508	Weighted mean of doublets (Accepted)
M6209-DM	5.4495	Weighted mean of all lines (Accepted)
	5.4519	Weighted mean of doublets
	5.4466	Refined by a $\sin^2 \theta$ method
Literature:	5.4505	Giesecke and Pfister
	5.447	Goldschmidt
	5.436	Wyckoff

NOTE: It appears that a value of a_0 in the order of $5.4500 \pm 0.005 \text{ \AA}$ is very close to the true value.

Tentative measurements of resistivity of these needles were made. Contacting was by silver paste on copper laminate mounts. This contacting indicates fairly uniform resistivities of approximately $1 \times 10^6 \text{ ohm-cm}$. The resistivities were not greatly sensitive to light.

Epitaxial Growth:

Based on the excellent results in synthesizing gallium phosphide and observations of the dendritic needle growth, use of the same general system appeared promising for epitaxy. The general system is illustrated in Figure 26. Principal modifications include:

- (a). A fused silica boat, partitioned, to place the Ga_2O_3 closely adjacent to the gallium arsenide substrates, yet separate to insure growth from the vapor phase only.
- (b). A heat sink arranged to insure the substrates being the coolest surface in the vicinity of the synthesis area.
- (c). Provisions to move the entire boat into and out of the hot zone.
- (d). Appropriate instrumentation for temperature measurement.

The synthesis-growth operation was carried out in a 30 mm I.D. fused silica tube, housed in a multiple zone furnace. Substrate wafers and a few grams of Ga_2O_3 were placed in the separate compartments of the rectangular boat but retained outside the furnace while initial heating was done. A few grams of red phosphorus was placed in a silica boat and retained outside the furnace until stabilized temperatures were accomplished. The system was purged with dry argon and hydrogen. The heat sink was adjusted to obtain approximately 850°C substrate temperature. The phosphorus was inserted in the 400°C zone and growth carried out under very low hydrogen flow rate for two hours. The phosphorus boat was then retracted, hydrogen flow rates increased and the furnace turned off for cooling.

A yellow powder deposit was observed on two of the three specimens. It was easily wiped off and did not appear to erode or damage the surfaces. Surfaces were smooth and lustrous with little evidence of staining and appeared gray in color to the naked eye.

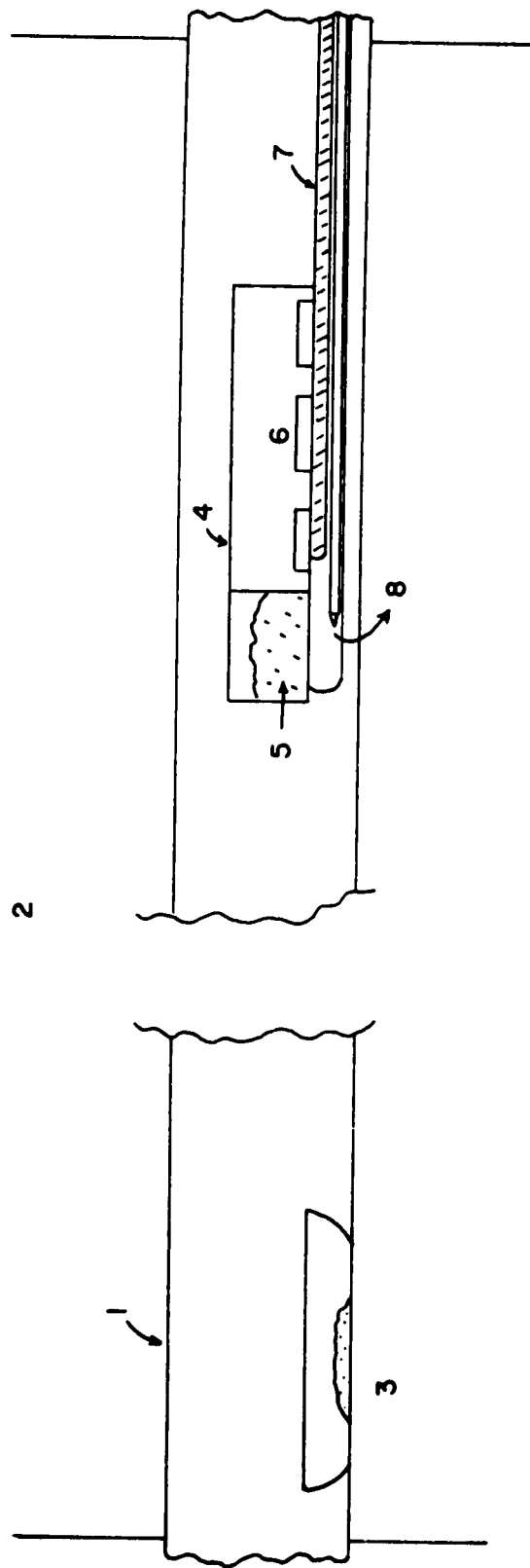


Figure 26. Epitaxial Growth System using Ga_2O_3 and Phosphorus Vapor.

1. Quartz Tube
2. 3-Zone Furnace
3. Phosphorus Charge
4. Quartz Boat Welded on Quartz Tube
5. Ga_2O_3 Charge
6. GaAs Wafers
7. Copper Heat Sink Inside Quartz Tube
8. Thermocouple Inside Quartz Tube

Microscopic examination was made of a cross sectioned wafer. An orange-colored layer was observed. Rigorous etching in $\text{KOH-H}_2\text{O}_2$ did not significantly affect this layer although the underlying gallium arsenide was severely attacked. A specimen, M6211-BN, was submitted for x-ray determination of structure. The Laue pattern obtained is illustrated in Figure 27. Exposure was made at approximately 15° from perpendicular to the surface and produced the typical 1:1:1 three-fold symmetry. No evidence of mixed phases was observed. Since the unit cell dimensions of gallium arsenide and gallium phosphide are so similar, positive identity of gallium phosphide requires direct comparison of halves of the same wafer, one with gallium phosphide growth.

Based on microscopic examination, however, the identity as gallium phosphide appears rather certain.



Figure 27. Laue Pattern of Epitaxial Surface of Specimen M6211-BN.

Epitaxial Growth by Iodine Transport:

An exploratory trial was made of epitaxial growth of gallium phosphide on gallium arsenide substrates, using the previously described gallium phosphide needles as source material, and the iodine transport method. The substrates, source, and elemental iodine were sealed in a quartz ampoule under vacuum. The ampoule was placed in a multiple-zone furnace and a suitable temperature gradient imposed. Figure 28 illustrates the salient features of the experiment. Substrate temperature was 700°C, source temperature was 850°C, and time of growth extended to two hours. Cognizance was taken that this schedule would involve growth of greater than the desirable thickness. Two specimens were used; one was broken in opening the ampoule.

Microscopic examination of the other indicated growth was accomplished. A yellow-orange translucent layer was observed under polarized light.

Subsequently epitaxial layers were grown using the iodine transport method, with zinc iodide as both the iodine source and dopant. A further modification was the use of 1000°C source and 750°C substrate temperatures. A few milligrams of high purity phosphorus was included in the ampoule, physically placed in - or on - the gallium phosphide source.

Results were very good; clear, yellow-orange gallium phosphide layers of 6 to 30 microns depth were grown. Figure 29 illustrates one specimen.

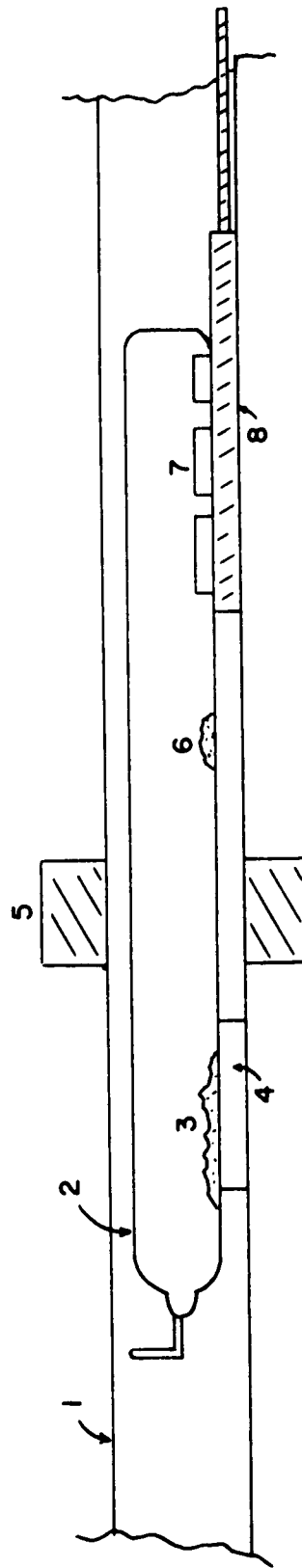


Figure 28. Iodine Transport Epitaxy System.

1. Quartz Tube
2. Sealed Ampoule
3. Gallium Phosphide Charge
4. Quartz Support
5. Insulating Ring
6. Iodine
7. Gallium Arsenide Wafers
8. Copper Heat Sink



Figure 29. Epitaxially Grown GaP Layer on GaAs by Iodide Transport.
(400x)

The specimens of epitaxy by the Ga_2O_3 -phosphorus were of n-type GaP on n-type GaAs. Bulk net carrier concentration of GaAs was $2 \times 10^{16}/\text{cc}$. The GaP layer (grown without intentional doping) was of the order of 10^{17} atoms/cc net carrier concentration. This effort was intended only to explore the epitaxial growth process; subsequent growth experiments were carried out by the iodide technique, which offered lower substrate temperature requirements. The substrate temperature is important in the growth of "p" GaP on "n" GaAs, since appreciable in-diffusion of zinc into the GaAs may occur during the growth of GaP.

It was proved advantageous to insert the ampoule, charge end first, into the previously stabilized furnace; this method results in better control. With source temperature of 1000°C, substrate temperatures of 750°C, an initial period of 15 minutes was required for ampoule and contents to come to temperature and achieve chemical equilibrium of the iodide products. Thus, an epitaxial run removed at the end of 15 minutes indicates only the beginning of epitaxial growth; at the end of 30 minutes growth of 6 to 8 microns was observed regularly.

Measurements of layer depth was accomplished by potting the wafer in Lucite or Epoxy, cross-sectioning and polishing. Edge lighting of the wafer produces dramatic illumination of the gallium phosphide layer and allows accurate microscopic measurements.

Initial iodide transport efforts were carried out with no dopant included, to obtain some control of the growth process; subsequently zinc iodide was included to produce "p" GaP layers. Brief discussion is in order of this "p on n" type of structure. The "n" gallium arsenide bulk material was exposed at the bottom by lapping, contact made by electroplated nickel, and coated with solder. The epitaxial surface was cleaned and contacted either by electroplated nickel, or ultrasonically applied Zn-In-Pb alloy. The GaP depth involved in these measurements averaged 10-microns and were grown in 30 minutes.

Epitaxial Device Parameters:

Photovoltaic output of the epitaxial units was disappointing and varied considerably, as indicated in Table VIII.

TABLE VIII

	<u>Device EG-35-2</u>	<u>Maximum Observed</u>
V _{oc}	0.52 Volts	0.8 Volts
I _{sc}	1.5 ma.	2.5 ma.
I _{sc} /cm ²	3.0 ma.	4.0 ma.

Diode characteristics of these junctions were observed by the curve tracer method. Two examples are illustrated in Figure 30.

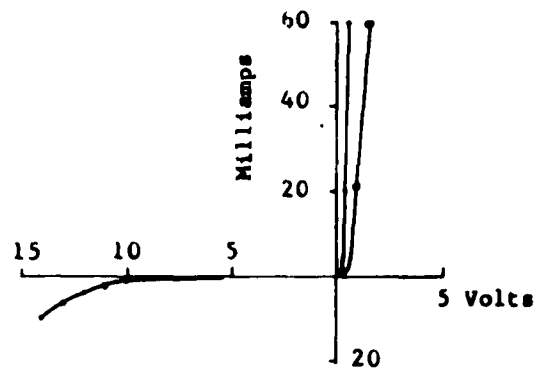


Figure 30. Epitaxial Device Diode Characteristics.

Spectral response of a typical unit (EG-35-2) is illustrated in Figure 31.

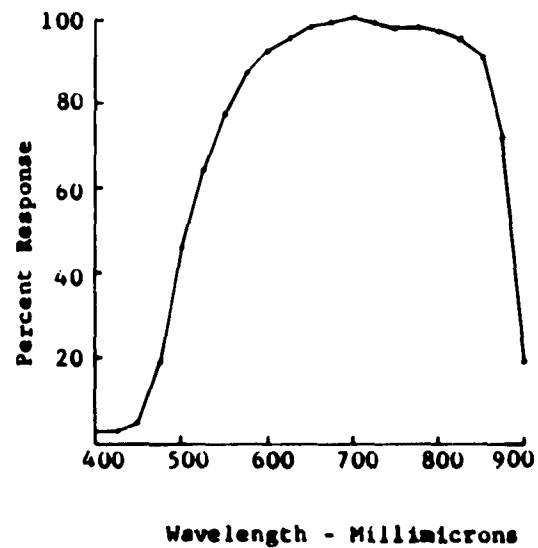


Figure 31. Spectral Response of Typical Epitaxial P-on-N Device, (EG-35-2)

Discussion:

The photovoltaic results measured on the epitaxial devices were disappointing. One could expect to observe V_{oc} of the order of 1-volt or more, for a good junction in gallium phosphide. The layers were regularly clear and highly translucent, of excellent crystalline structure as defined by Laue patterns. Carrier concentrations in the gallium phosphide were estimated at 10^{18} atoms/cc, a trifle low for good conversion efficiency, but not so poor as to reflect in low V_{oc} . The diode characteristics indicate a junction with graded rather than abrupt characteristics. The spectral response is indicative of a shallow junction in GaAs. Retrogressing briefly, the substrate temperature was 750°C, growth time 30 minutes, with a zinc environment, which establishes the necessary conditions for significant zinc diffusion into GaAs during the growth process.

Based on the foregoing evidence, it is considered that the photovoltaic data reflect the presence of a diffused junction within the GaAs substrate, rather than coincident with the GaP-GaAs interface. This inference is substantiated by the observed relation between photovoltaic results and substrate doping. Photovoltaic performance was better with GaAs substrates of high net "n" carrier concentration, where zinc penetration would be somewhat slower.

The converse geometry, on "n" GaP on "p" GaAs was explored briefly. Growth of GaP, with elemental tin dopant, by the iodine process was carried out, using zinc doped GaAs substrates. The out diffusion of zinc from the substrates was observed to produce compensation of the GaP, producing poor

photovoltaic properties and very high surface resistivity (of the order of 10^7 ohms per square). Had time permitted, further exploration of this type was considered using tellurium as a dopant; a 2-step, heavily doped "n"-heavily doped "p" GaP epitaxy procedure was considered a promising concept.

The results reported here must be viewed as tentative; the epitaxial effort was a secondary, exploratory, small-scale effort, and not wide or rigorous in scope. Tentative comparison indicates the epitaxial structure is subject to peculiar fabrication difficulties with regard to junction placement, as is also the deep variable gap structure. Both structures may be amenable to improvement with further research. The physical growth process of the epitaxial surface is not unduly difficult, and is attractive in that it minimizes time-temperature cycles. Photovoltaic properties, although not dramatic in these early devices, are respectable and offer promise of significant improvement.

Electroluminescence:

The injection luminescence of both the single gap and variable gap structure was investigated as a possible tool for evaluating the device structure. It was accepted that due to the junction location in the variable gap devices being below the predominantly GaP areas, a similarity in luminescence might be expected.

Electroluminescent diodes were fabricated somewhat differently than the photovoltaic counterpart. To achieve high current density, mesa-type structures were considered. Discrete fabrication steps are indicated in Table IX.

TABLE IX

Fabrication Steps and Sequence-Electroluminescent Diodes.

	<u>Single Gap</u>	<u>Variable Gap</u>
Step:		
Wafering, lapping, chemical polishing,	X	X
Phosphorus Diffusion 900°C - 15 Atm. - 6 hours,		X
H/F cleaning, rinsing, drying,		X
*Zinc Diffusion 800°C - 10 minutes,	X	X
Mask out dot pattern, plate nickel, coat solder,	X	X
Lap bottoms, clean, plate nickel, coat solder,	X	X
Chemically etch mesas,	X	X
Scribe, cleave mesas, mount on TO-5 bases,	X	X
Final cleaning and drying,	X	X
Evaluation for luminescence,	X	X

NOTE: * - The emission intensity as a function of junction depth was determined in a brief study to be optimum with a depth of approximately 8 microns, produced by this diffusion schedule.

Diode characteristics of these mesa-type diodes were characteristically good, as previously indicated in Figure 6. The reverse breakdown voltage for the variable gap specimen were regularly about fourteen volts, some were observed to exceed this figure significantly. Forward characteristics were very steep, with total series resistance less than 1-ohm for both types.

Junction depth was measured microscopically by etch stain techniques. The variable gap structures had junctions coincident with the bottom of the GaP layer. Detection of emitted light was by means of a silicon solar cell, with the emitting junction 0.125 inch from its surface. Delivery of photo-multiplier detection and measuring equipment was delayed and this system employed for the sake of expediency. Admittedly, the results are considered qualitative only.

Mesa diameters were held closely to 1-mm. No reflection devices were used, direct junction edge emission only was measured. Excitation was accomplished by direct current pulse techniques and measurements of current by display of the voltage drop across a precision 1-ohm resistor on a Tektronix Model #535 scope. Detected emission was measured similarly as the I_{sc} of the silicon solar cell. Both measurements were at 25°C. The specified conversion efficiency of 10 percent was used to mathematically derive the rate of photon emission. Since the efficiency of the detector at wavelength greater than 0.9 microns is known to be less than with solar spectrum input, the values thus obtained are surely conservative. Wavelength emission of the GaAs junctions are documented in the literature⁽⁵⁾; emission from the variable gap structure is of extreme interest, but was delayed pending the sensitive detection equipment.

Qualitatively, the variable gap and single gap structures exhibited similar emission efficiencies. Best results are tabulated as follows:

	<u>Input Current/μm^2</u>	<u>Detected I_{ph}, Micro-amps.</u>	<u>Photon/Sec.</u>
Single Gap,	150 μm^2	12	7.5×10^{14}
Variable Gap,	150 μm^2	11	7.0×10^{14}

Considering the effective area, and depth, of emission aperture from the junction in relation to the current carrying area of the junction, the probable quantum efficiency is indicated to be a few percent in either case. This is in general agreement with data given in the literature⁽⁵⁾. It is considered that the similarity in luminescence is primarily due to the similar placement of the junction.

V. SUMMARY

Significant improvement in device uniformity and quality was achieved by the chemical polishing technique developed in the course of this investigation.

Acceptable ohmic contacting procedures are described for GaAs and GaP surfaces.

Shallow depth variable gap devices, with junction depths of the order of 3-microns were fabricated with essentially equal photovoltaic properties as the conventional single gap GaAs devices. These devices indicate spectral response broadened in the blue region, increased ruggedness, and a small numerical advantage in temperature performance.

Deep variable gap structures of competitive but smaller photovoltaic efficiencies were achieved by minimizing or elimination of heavy compensation effects from phosphorus impurities. Significant difference in spectral response was observed. Further differences of importance are implied with the advent of junction placement within the GaP region.

Synthesis of GaP was carried out by two methods. Acceptable product purity was obtained with reasonable effective yield. Melt grown ingots of gallium phosphide were produced, and used as source material for epitaxial growth of GaP on GaAs substrates.

Epitaxial layers were grown successfully, with fairly good control and uniformity. Two methods were explored and the iodine transport method is considered the better. P-on-N structures were produced and tested. A difficulty in restricting intra-diffusion from the p-type GaP into the substrate was exposed.

Electroluminescent mesa diodes of single gap and deep variable gap structures were fabricated and tested qualitatively. Results indicate a similarity in emission, considered the result of junction placement below the predominantly gallium phosphide region of the variable gap units.

VI. REFERENCES

- (1). Jackson, E. D., - Paper given at the Conference on Solar Energy, Tucson, Arizona. November, 1955.
- (2). Rappaport, Wysocki, Loferski - Tri-Annual Progress Report, December, 1958. Contract Nr. DA-36-039-SC-78184.
- (3). Stone, L.E., Medcalf, W.E., - Final Technical Summary Report, Oct. 10, 1960. Contract Nr. DA-36-039-SC-85246.
- (4). Keyes, - "Doping of Semiconductors for Injection Lasers", Proceedings of I.E.E.E., April, 1963. p. 602.
- (5). Henisch, - "Electroluminescence", Pergamon Press.
- (6). Stone, L.E. - "Conversion of Gallium Arsenide to Gallium Phosphide by Solid State Diffusion" - Jour. App. Physics. Sept., 1962.
- (7). Stone, L.E., Webb, Geo.N. - First Quarterly Technical Report, August 31, 1962. Contract Nr. DA-36-039-SC-89106.
- (8). Stone, L.E., Webb, Geo. N. - Second Quarterly Technical Report. Contract Nr. DA-36-039-SC-89106.
- (9). Stone, L.E., Webb, Geo. N. - Third Quarterly Technical Report. Contract Nr. DA-36-039-SC-89106.
- (10). Sullivan, Pompliano - Journal of Electrochem. 108, No. 3, 1961, p. 60-C.
- (11). Gerschenzon, Frosh, Mikulyak - "Precipitation in GaP", Abs. J. of Electrochem. May, 1961.
- (12). Papers presented at the Pittsburgh Meeting of Electrochemical Society. April 15, 16, & 17, 1963.
- (13). Third Quarterly Technical Report, The Eagle-Picher Company. Feb. 28, 1963. Contract Nr. DA-36-039-SC-89106.
- (14). "A Flow Synthesis of Gallium Phosphide, Etc." - Bodi, J. of Electrochem. Vol 109, No. 6.
- (15). Ritchie, E. J. - Joplin Research, The Eagle-Picher Company.

VII. PERSONNEL

Engineering Time Expended from May 1, 1962 to April 30, 1963:

Louis E. Stone,	1,704 Hrs.
George N. Webb,	1,916 "
William A. Ames,	113 "
J. S. Roderique,	472 "
Harold L. Allen,	37 "
Lloyd W. Brown,	132 "
John C. Budiselic,	312 "
Richard H. Fahrig,	44 "
Joseph E. Powderly,	65 "
Ralph J. Starks,	120 "
	<hr/>
Total,	4,915 Hrs.

LES/tp.

AD _____	Accessories No. _____	UNCLASSIFIED	AD _____	Accessories No. _____	UNCLASSIFIED
<p>The Eagle-Picher Company, Chemical & Metals Division, Miami, Oklahoma. VARIABLE ENERGY GAP DEVICES, L. E. Stone, Geo. N. Webb, J. R. Musgrave.</p>			<p>The Eagle-Picher Company, Chemical & Metals Division, Miami, Oklahoma. VARIABLE ENERGY GAP DEVICES, L. E. Stone, Geo. N. Webb, J. R. Musgrave.</p>		
<p>1. Variable Energy Gap Devices 2. GaP-GaAs Devices 3. Photovoltaic Devices 4. Signal Corps Contract Nr. DA-36-039-SC-89106 DA-36-039-SC-89106.</p>			<p>1. Variable Energy Gap Devices 2. GaP-GaAs Devices 3. Photovoltaic Devices 4. Signal Corps Contract Nr. DA-36-039-SC-89106 DA-36-039-SC-89106.</p>		
<p>Final Technical Summary Report - May 1, 1962 to May 1, 1963. 69 pages, Illus - Graphs. Signal Corps Contract Nr. DA-36-039-SC-89106</p>			<p>Final Technical Summary Report - May 1, 1962 to May 1, 1963. 69 pages, Illus - Graphs. Signal Corps Contract Nr. DA-36-039-SC-89106</p>		
<p>Gallium phosphide variable energy gap devices fabrication, evaluation, photovoltaic parameters. Synthesis of gallium phosphide. Epitaxial growth GaP on GaAs Electroluminescent diodes.</p>			<p>Gallium phosphide variable energy gap devices fabrication, evaluation, photovoltaic parameters. Synthesis of gallium phosphide. Epitaxial growth GaP on GaAs Electroluminescent diodes.</p>		

AD _____	Accessories No. _____	UNCLASSIFIED	AD _____	Accessories No. _____	UNCLASSIFIED
<p>The Eagle-Picher Company, Chemical & Metals Division, Miami, Oklahoma. VARIABLE ENERGY GAP DEVICES, L. E. Stone, Geo. N. Webb, J. R. Musgrave.</p>			<p>The Eagle-Picher Company, Chemical & Metals Division, Miami, Oklahoma. VARIABLE ENERGY GAP DEVICES, L. E. Stone, Geo. N. Webb, J. R. Musgrave.</p>		
<p>1. Variable Energy Gap Devices 2. GaP-GaAs Devices 3. Photovoltaic Devices 4. Signal Corps Contract Nr. DA-36-039-SC-89106 DA-36-039-SC-89106.</p>			<p>1. Variable Energy Gap Devices 2. GaP-GaAs Devices 3. Photovoltaic Devices 4. Signal Corps Contract Nr. DA-36-039-SC-89106 DA-36-039-SC-89106.</p>		
<p>Final Technical Summary Report - May 1, 1962 to May 1, 1963. 69 pages, Illus - Graphs. Signal Corps Contract Nr. DA-36-039-SC-89106</p>			<p>Final Technical Summary Report - May 1, 1962 to May 1, 1963. 69 pages, Illus - Graphs. Signal Corps Contract Nr. DA-36-039-SC-89106</p>		
<p>Gallium phosphide variable energy gap devices fabrication, evaluation, photovoltaic parameters. Synthesis of gallium phosphide. Epitaxial growth GaP on GaAs Electroluminescent diodes.</p>			<p>Gallium phosphide variable energy gap devices fabrication, evaluation, photovoltaic parameters. Synthesis of gallium phosphide. Epitaxial growth GaP on GaAs Electroluminescent diodes.</p>		